

Image Cover Sheet

CLASSIFICATION

UNCLASSIFIED

SYSTEM NUMBER

25555



TITLE

A PROCEDURE FOR MEASURING THERMAL EMISSION SPECTRA AT AMBIENT
TEMPERATURE

System Number:

Patron Number:

Requester:

Notes:

DSIS Use only:

Deliver to: JR



RESEARCH AND DEVELOPMENT BRANCH
DEPARTMENT OF NATIONAL DEFENCE
CANADA

DEFENCE RESEARCH ESTABLISHMENT OTTAWA

DREO REPORT NO. 708
DREO R 708

A PROCEDURE FOR MEASURING THERMAL EMISSION SPECTRA AT AMBIENT TEMPERATURE

by

B.G. Young and R.J. Brown



PROJECT NO.
38-80-07

JANUARY 1975
OTTAWA

CAUTION

This information is furnished with the express understanding that proprietary and patent rights will be protected.

RESEARCH AND DEVELOPMENT BRANCH

DEPARTMENT OF NATIONAL DEFENCE
CANADA

DEFENCE RESEARCH ESTABLISHMENT OTTAWA

REPORT NO. 708

A PROCEDURE FOR MEASURING THERMAL EMISSION SPECTRA
AT AMBIENT TEMPERATURE

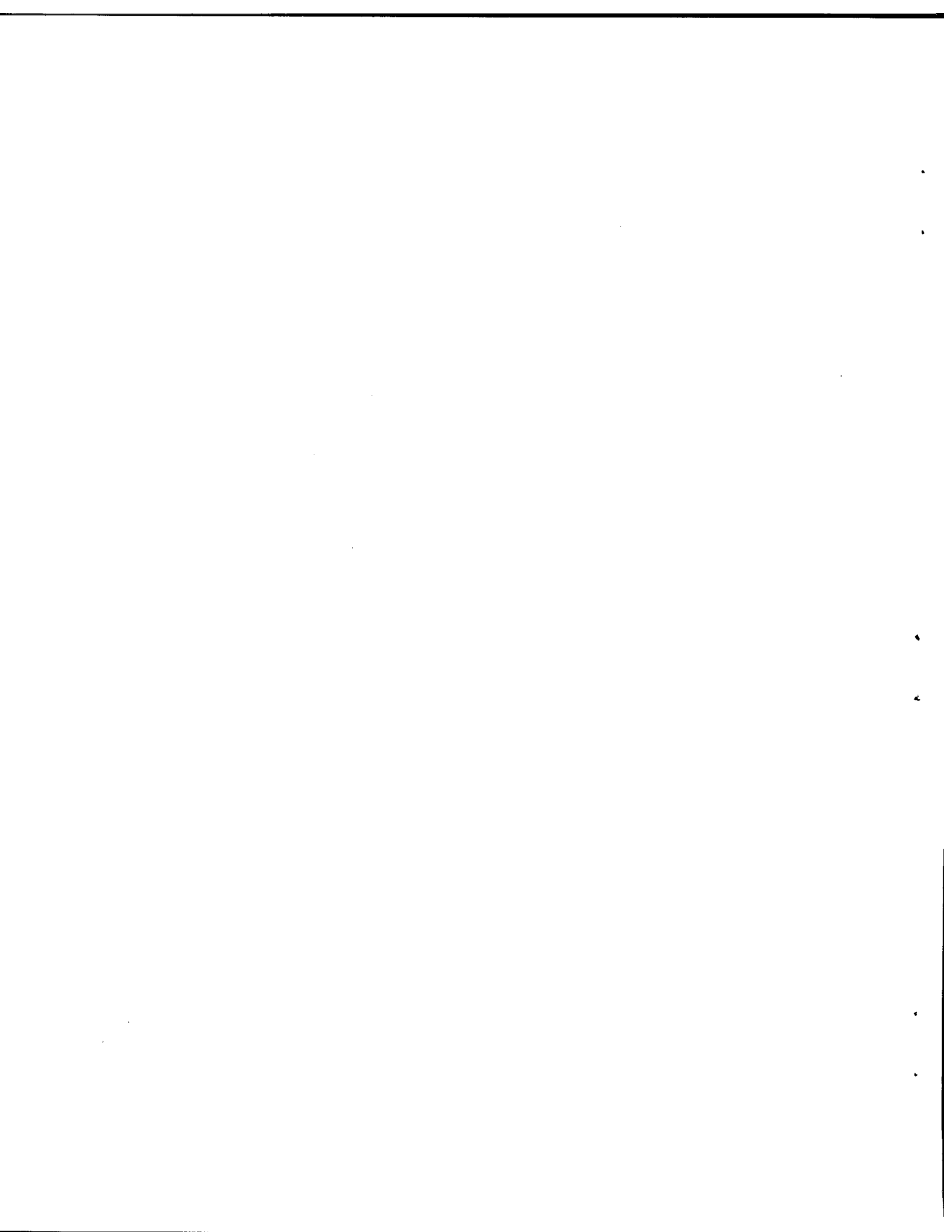
by

B.G. Young and R.J. Brown

Remote Sensing Section
Earth Sciences Division

PROJECT NO.
38-80-07

RECEIVED DECEMBER 1974
PUBLISHED JANUARY 1975
OTTAWA



ABSTRACT

This report describes the preliminary work to collect the infrared spectral emission signatures of ambient temperature objects using a Fourier transform spectrometer operating in the 8 - 13 micrometer wavelength range. Details of the construction of a sample container are presented along with a description of the spectrometer, the controlling computer, and the data collection techniques and procedures. A system test, which is actually the ratio of two blackbodies at different temperatures, suggests that these procedures are valid. The emissivities of Krylon 1602 ultra-flat black paint, crushed fused quartz, and three types of cotton are presented.

RÉSUMÉ

Le présent rapport décrit les travaux préliminaires permettant de recueillir des signatures d'émission-spectrale dans l'infrarouge d'objets à la température ambiante, au moyen d'un spectromètre à transformateur de Fourier, fonctionnant dans la plage de longueur d'onde de 8 à 13 micromètres. Des détails sur la construction du contenant à spécimen sont présentés de même que la description du spectromètre, de l'ordinateur de contrôle et des techniques et méthodes d'obtention des données. Une vérification du système, consistant à faire le rapport de l'émission de deux corps noirs de différentes températures, tend à montrer la validité de ces méthodes. Les émissions de la peinture noire ultra-mate, du quartz fusionné et écrasé, et de trois types de coton sont présentées.

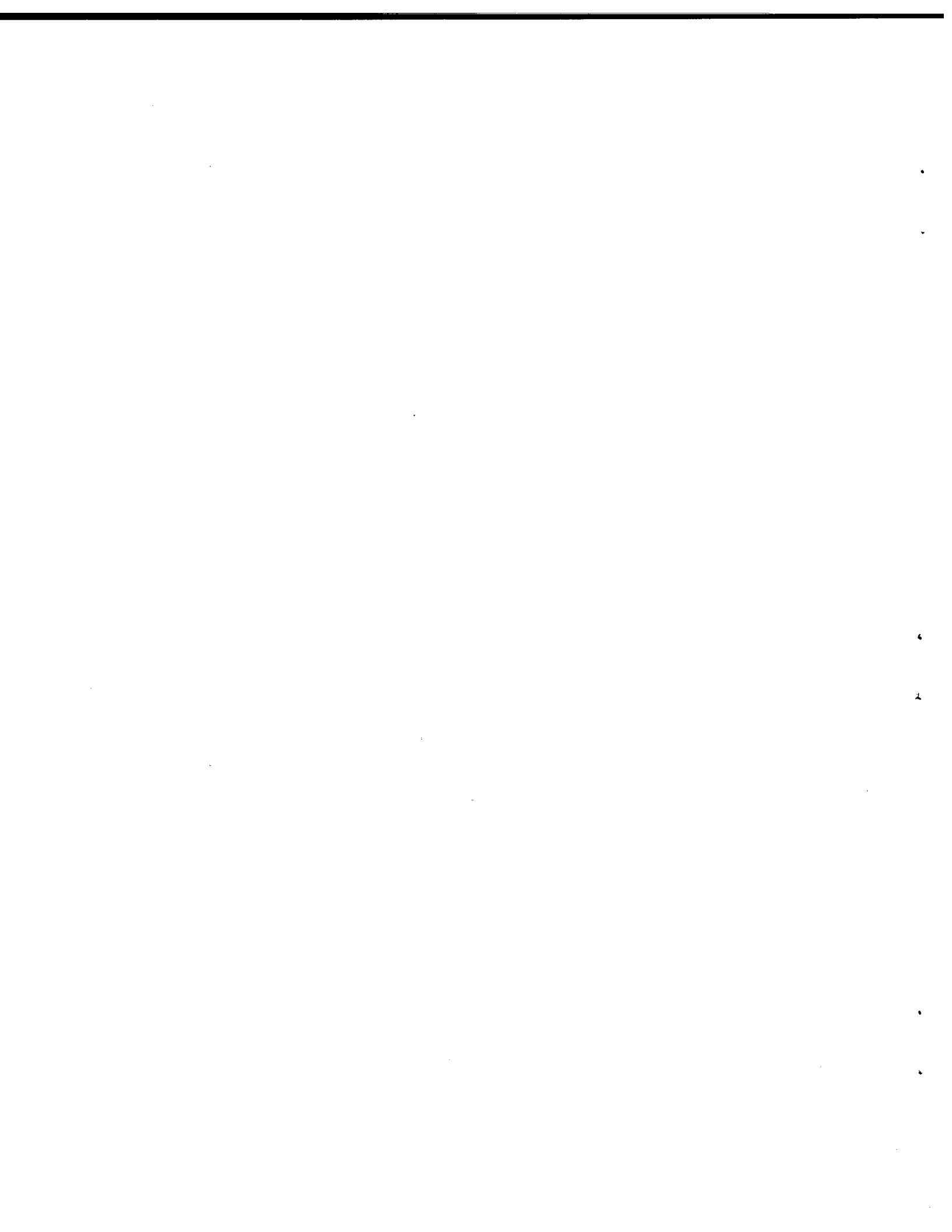


TABLE OF CONTENTS

	<u>Page</u>
<u>ABSTRACT/RÉSUMÉ</u>	iii
<u>TABLE OF CONTENTS</u>	v
<u>INTRODUCTION</u>	1
<u>RADIATION THEORY</u>	3
<u>THE SPECTROMETER</u>	5
SELECTING THE SPECTROMETER	5
FOURIER SPECTROSCOPY	8
MODIFICATIONS TO THE SPECTROMETER	14
<u>SAMPLE AND SAMPLE ENVIRONMENT</u>	14
COLD BOX DESIGN PARAMETERS AND DESIGN CRITERIA	14
SAMPLE -- INSTRUMENT INTERFACE	17
COLD BOX CONSTRUCTION	17
RADIATION SOURCES	19
<u>THE BLACKBODY SOURCE</u>	19
<u>INSULATED BLACK SOURCE</u>	22
<u>SAMPLE SUBSTRATE</u>	22
<u>ALIGNMENT SOURCE</u>	23
<u>REFLECTING SOURCE</u>	23
COLD BOX ACCESSORIES	23
<u>NITROGEN GAS GENERATOR</u>	23
<u>LIQUID NOTROGEN PUMP</u>	24
<u>SPECTROMETER SOFTWARE</u>	25

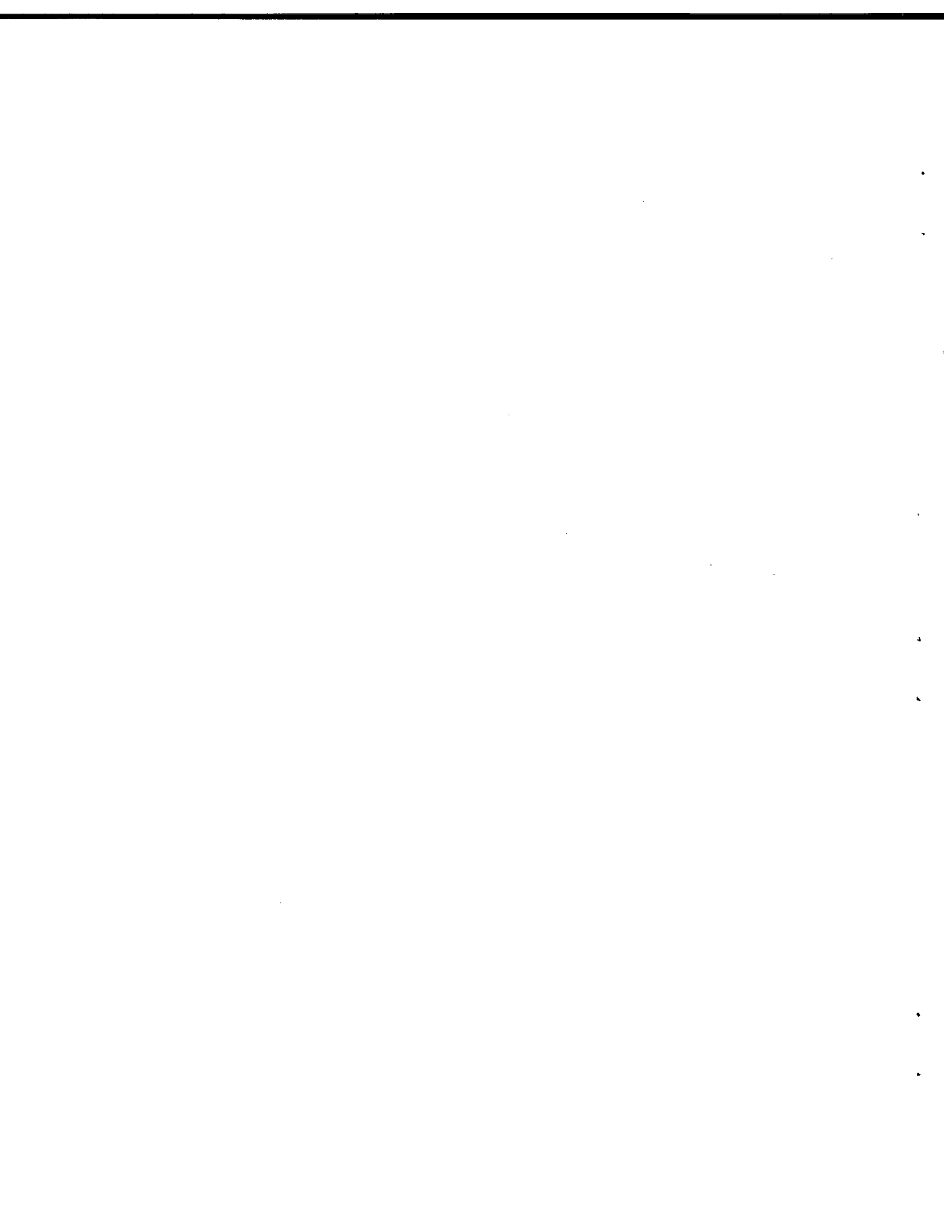


TABLE OF CONTENTS - Continued

	<u>Page</u>
GENERAL DESCRIPTION OF COMPUTER AND PERIPHERALS	25
THE FTS - 14 OPERATING SYSTEM	27
<u>SCAN ADDITION</u>	27
<u>FOURIER TRANSFORMATION</u>	27
<u>APODIZATION FUNCTION</u>	27
<u>PHASE AND COMPENSATION ERRORS</u>	28
<u>FILE SUBTRACTION</u>	28
<u>PLOTTING DATA</u>	29
<u>ALARM SIGNALS</u>	29
<u>DATA ACQUISITION</u>	30
EMISSIONITY CALCULATIONS	30
<u>GENERAL FORM OF EMISSIONITY EQUATION</u>	30
<u>PARAMETERS REQUIRED TO SOLVE THE EMISSIONITY EQUATION</u>	31
<u>SOLUTION OF EMISSIONITY EQUATION</u>	32
<u>SOFTWARE REQUIRED</u>	36
<u>COLD BOX PROFILE FUNCTION</u>	36
<u>OPERATING TECHNIQUES</u>	38
DETERMINING EQUILIBRIUM TEMPERATURE	39
TEST OF THE SYSTEM	39
<u>TEMPERATURE GRADIENT ACROSS AN INSULATED SAMPLE</u>	39
<u>TOTAL SYSTEM TEST</u>	40
TEMPERATURE GRADIENT BETWEEN THE SURFACE OF AN INSULATED SAMPLE AND THE ALUMINUM SUBSTRATE	40
<u>RESULTS</u>	42

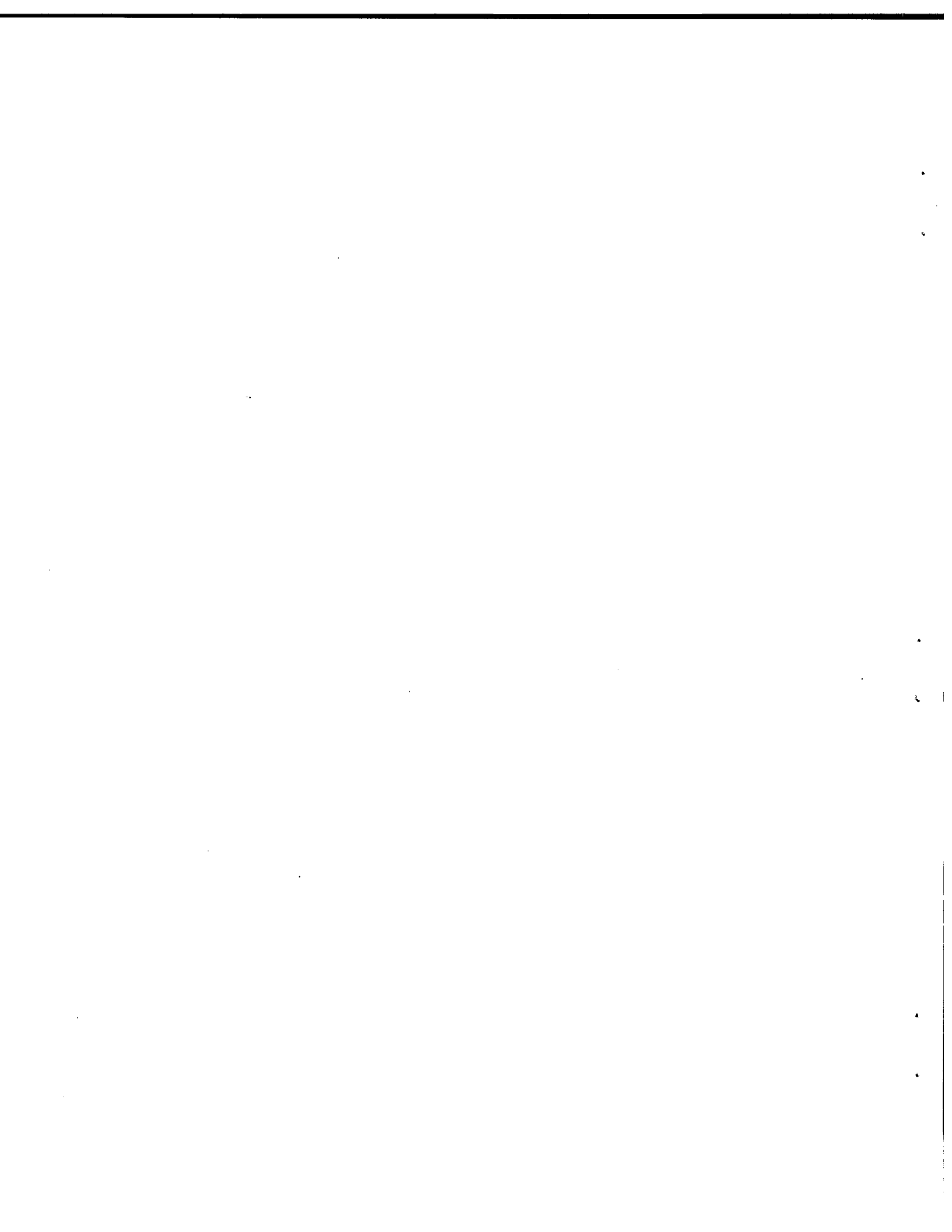


TABLE OF CONTENTS - Continued

	<u>Page</u>
GENERAL	42
KRYLON 1602 ULTRA-FLAT BLACK PAINT	42
<u>SPECIMEN PREPARATION</u>	42
<u>KRYLON EMISSIVITY</u>	42
CRUSHED FUSED QUARTZ	43
<u>SAMPLE PREPARATION</u>	43
<u>EMISSIVITY OF CRUSHED QUARTZ</u>	43
COTTON	45
<u>SAMPLE PREPARATION</u>	45
<u>EMISSIVITY OF COTTON</u>	45
<u>CONCLUSIONS</u>	45
<u>REFERENCES</u>	48



INTRODUCTION

This report describes preliminary work in an investigation to collect infrared spectral emission signatures in the 8 to 13 μm region of the electromagnetic spectrum and to assess what changes occur in these due to environmental factors. It is hoped that this information may be useful in a remote sensing target detection scheme.

To date most target detection approaches have been based on the analysis of fixed outputs of multispectral scanners (MSS), infrared line scanners (IRLS), or forward looking infrared scanners (FLIR). It is our feeling that such analysis would be much more effective if the choice of channels were based on a knowledge of the spectral signatures of targets and backgrounds. To date few imaging MSS even divide the 8 to 13 μm region into separate spectral channels. However, two notable exceptions are the NASA 24-channel scanner (1) and the Honeywell multilayer detector sandwich (2).

To meet our goals we intend first to measure emission signatures in the 8 to 13 μm region of the electromagnetic spectrum in the laboratory. Then we intend to measure these same signatures in the field in order to assess the degradation which results from propagation through the atmosphere and from other environmental factors such as dew or frost which can substantially alter spectral emission signatures (3).

This particular region of the spectrum was chosen because:

- (a) the blackbody spectral emission curves of ambient temperature objects peak in this region.
- (b) emission predominates over reflection in this region (in fact it does so at wavelengths greater than about 3.5 μm (4)).
- (c) this band corresponds to a region of high atmospheric transmission. Figure 1, which is a plot of the atmospheric transmittance for a 6000 ft. horizontal path at sea level, shows two main 'atmospheric windows' extending from about 3 to 5 μm and 8 to 13 μm .
- (d) there are gaps in the spectral data within the chosen region.

Until recently the measurement of emission spectra from surfaces at ambient temperature has been restricted by the low sensitivity of conventional dispersion spectrometers in the infrared. Hence workers have resorted either to the calculation of emission spectra from measured reflection spectra using an extension of Kirchoff's law (5,6,7,8,9) or to the measurement of emission spectra from surfaces which were much warmer than ambient (10, 11). These techniques were adequate for the study of surface properties

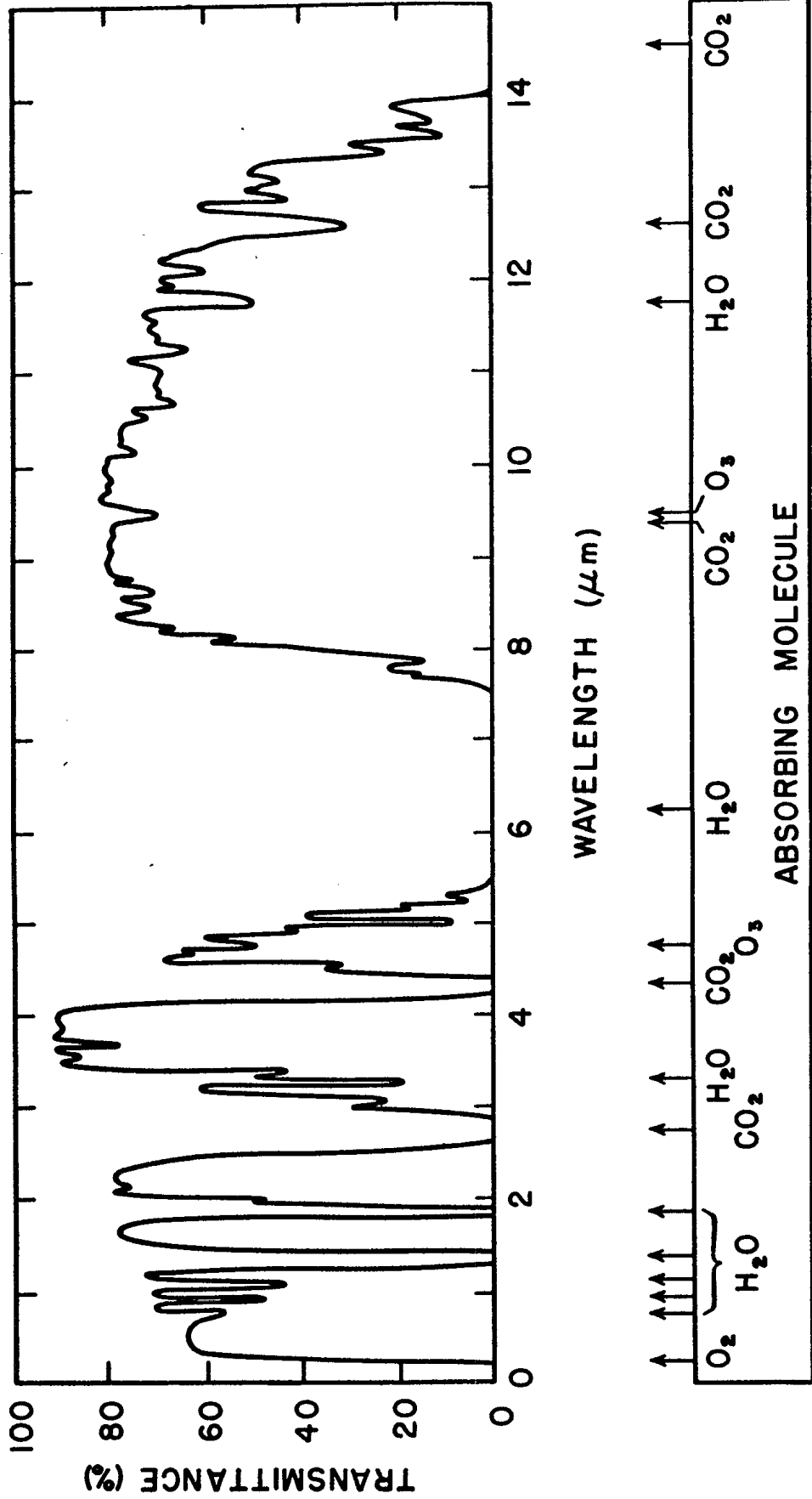


Fig. 1. Transmittance of the atmosphere in the region 0 to 15 μm for a 6000 ft. horizontal path at sea level containing 17 mm of precipitable water.

of materials, but not for the study of the degradation of emission spectra by environmental factors, which is a principal purpose of the present series of experiments.

During the past decade there has been a significant improvement in the capability of commercial infrared spectrometers to measure spectra from sources which have weak or variable intensity (12). This improvement is due to the development of better detectors (13) and to the availability of digital computers which can perform rapid and accurate Fourier or Hadamard transforms. In fact spectrometers of the Fourier interferometer type have been flown on aircraft, and satellites (14, 15, 16, 17) and the feasibility of using such instruments to measure the emission spectra of the earth has been demonstrated. Hence, a Fourier transform spectrometer was chosen to collect emission spectra in the work outlined.

This report describes the equipment, procedures for collecting spectral signatures in the laboratory, and computational methods and presents some representative spectral signatures. The equipment is presently being modified to permit carrying out degradation experiments and this work will be reported at a later date.

RADIATION THEORY

The emission from an object at a given temperature T is characterized by its emissivity, ϵ_λ , which is defined by:

$$\epsilon_\lambda = \frac{N_\lambda(T)}{N_\lambda^b(T)} \quad (1)$$

where $N_\lambda(T)$ = the spectral radiant emittance of the object at temperature T

and $N_\lambda^b(T)$ = the spectral radiant emittance of a blackbody at temperature T

The properties of blackbody radiation will not be presented here as there are many standard text books, such as Hudson (18), which have excellent sections on this topic.

However, we would like to emphasize an interesting property of materials which was discovered experimentally by Kirchoff. He found that for any object

$$\frac{N_\lambda(T)}{\alpha_\lambda} = N_\lambda^b(T) \quad (2)$$

where α_λ = the absorptance of the object.

This equation is of the same form as that defining the emissivity of an object and hence

$$\epsilon_{\lambda} = \alpha_{\lambda} \quad (3)$$

Furthermore, for an opaque body, it follows from the principle of conservation of energy that the emissivity and reflectivity, r_{λ} , are related by

$$\epsilon_{\lambda} = 1 - r_{\lambda} \quad (4)$$

Hence, a knowledge of one of these quantities allows determination of the other.

In general the emissivity or reflectance of an object is a function of the angle of view as measured from the normal to the sample surface. For a perfectly diffuse reflector, the reflected flux at any angle of view is proportional to the cosine of this angle. This relationship is known as Lambert's cosine law and such a diffuse reflector is known as a Lambertian surface. This same relationship holds for the radiant emittance from a perfectly diffuse surface. But since the projected area of a sample perpendicular to the viewing direction is proportional to the cosine of this angle the radiant energy from a Lambertian surface per unit area perpendicular to the viewing direction is independent of this angle.

A blackbody follows Lambert's law exactly and consequently its emissivity is not a function of the angle of measurement. Many bodies also follow this law closely, especially for viewing angles less than 60° from the normal. However, in general, a body will not be a diffuse reflector and its emissivity will be a function of its surface properties, being therefore, dependent on such parameters as particle size, packing, and surface roughness. This dependence is quite complicated as different spectral features may either increase or decrease as particle size is decreased (6). In fact a continuing reduction in particle size may even reverse a trend in a particular spectral feature (19). However, despite these complications it has been possible to identify particulate matter using remote spectroscopy (20). Furthermore, it should be noted that for a good emitter such as water the depth of the surface layer contributing to the observed emission energy in the infrared region of the spectrum is approximately equal to ten micrometers (21, 22).

The emission spectra of gases, liquid and solids differ considerably. In gases, emission spectra are due to transitions between bound molecular energy levels of which there are three types: electronic, rotational and vibrational. Large energies are required for transitions between electronic states corresponding to spectra in the ultra-violet, visible and near infrared portions of the electromagnetic spectrum. Transitions between rotational levels yield radiation in the far infrared while those between vibrational states correspond to spectra in the infrared region under consideration in this paper. Actually, the transitions which we are measuring are between vibrational-rotational levels which are the result of the superposition of rotational levels on the vibrational one (23).

In order for absorption and hence emission to occur at a particular wavelength there must be a means of coupling the radiation to the particular

vibrational-rotational mode. This is done through the electric dipole moment. That is, only those transitions absorb or emit electromagnetic radiation which have an oscillating dipole moment associated with them.

The absorption and emission spectra of solids and liquids differ from those of a gas due to density differences. In a gas the effect of neighbouring molecules is slight and the spectra consist of series of distinct pressure-broadened lines corresponding to the transitions within the molecules. However, as the density of the material increases the number of molecular collisions and hence interactions increase. The result is that the previously distinct lines in the vibrational-rotational spectrum become broadened, smeared, and finally disappear altogether. As in the case of molecular spectra the emission spectra of a solid is not its vibrational spectrum but only those modes which can be coupled to incoming or outgoing electromagnetic radiation through an oscillating dipole moment. A thorough discussion of vibrational selection rules in solids is given by Carter (24).

Both gaseous and solid emission and absorption spectra were encountered in the present work. The emission from a sample is of course that from a solid but the subsequent transmission through the atmosphere will result in absorption and emission at the wavelength corresponding to transitions within the gas molecules along the propagation path.

THE SPECTROMETER

There have been many excellent reviews which compare spectrometric systems or describe advances in the measurement of the thermal infrared spectra, (see, for example, the papers from the Aspen Conference of 1970(5)). Consequently we will not attempt to present a history of these developments. Instead, the criteria which led to the selection of the Fourier transform spectrometer for the present experiment are outlined and this instrument is described in sufficient detail for an understanding of the data acquisition and processing techniques.

SELECTING THE SPECTROMETER

The intention was to measure the spectral radiance from a target or background material at ambient temperatures in the field. It is assumed that the surface area of the material is large enough to fill the field of view of the spectrometer. Ambient temperatures vary widely but a 'normal' temperature for the present purpose might lie within the range 233 K to 313 K. Stefan's law shows that the peak spectral radiance varies by more than a factor of four over this temperature range and we arbitrarily specified a signal-to-noise ratio greater than 100 for a blackbody at 273 K.

The bandwidth of the spectrometer should extend over the 3 to 5 μm and the 8 to 13 μm atmospheric windows. However, photon detectors of the necessary detectivity have too narrow a usable bandwidth to measure spectra in both windows simultaneously and consequently two detectors are needed to cover the full range from 3 to 13 μm . At the beginning of the experiment in 1971 the preferred detectors were HgCdTe for the 8 to 13 μm band and InSb for the 3 to 5 μm band, both of which operate at the convenient temperature of liquid nitrogen (77 K). The HgCdTe detector was chosen which in effect limited the spectral region of investigation to the 8 to 13 μm band.

To delay obsolescence of the data and to permit better identification of molecular absorbers and emitters in the atmosphere a spectral resolution of 1 cm^{-1} (.01 μm at 10 μm) was specified which is substantially better than that which can presently be attained with a multi-spectral scanner.

Environmental conditions can change rapidly during field measurements and it should be possible to collect a spectrum in a period no longer than a few minutes. Briefly, then, the spectrometer should measure within a few minutes the radiance from an extended blackbody at 273 K at a resolution of 1 cm^{-1} and with a signal-to-noise ratio greater than 100.

The overall sensitivity of a spectrometer may be expressed by the signal-to-noise, s/n , (see for example, Hanel (26) or Stair (27)) as

$$s/n = \eta N_{\nu}^b(T) \Delta\nu \theta \tau^{-\frac{1}{2}} A_d^{-\frac{1}{2}} D^* \quad (5)$$

where η = the efficiency of the system, including modulation efficiency and transmission losses.

$N_{\nu}^b(T)$ = the spectral radiance in $\text{W}/(\text{cm}^2 \text{sr cm}^{-1})$
 ($N_{\nu}^b(T)$ becomes the noise equivalent spectral radiance, NESR, when $s/n = 1$)

$\Delta\nu$ = the spectral resolution in wavenumbers, cm^{-1}

$\theta = A \Omega$ is the throughput, where A and Ω are the area and solid angle of the entrance aperture, in $\text{cm}^2 \text{sr}$

τ = the integration time in sec.

A_d = the detector area in cm^2 .

D^* = the detectivity of the detector in $\text{cm Hz}^{\frac{1}{2}}/\text{W}$.
 (The use of D^* in equation 5 assumes that the instrument is detector noise limited and this is usually true in the infrared).

Four of these parameters were specified by the problem; i.e. $s/n > 100$, $\tau < 60$ sec, $\Delta\nu = 1 \text{ cm}^{-1}$ and $N_{\nu}^b(T)$, the spectral radiance from a blackbody at 273 K. The latter is given by Planck function,

$$N_{\nu}^b(T) = C_{1\nu}^3 / \pi (e^{C_{2\nu}/T} - 1) \text{ W}/(\text{cm}^2 \text{sr cm}^{-1}) \quad (6)$$

where $C_1 = 3.7403 \times 10^{-12}$ (W cm²)

and $C_2 = 1.43848$ (cm K)

Hence the spectral radiance at 1000 cm⁻¹ (10 μm) is

$$N_{1000}^b(273) = 6.18 \times 10^{-6} W / (\text{cm}^2 \text{ sr cm}^{-1}). \quad (7)$$

The detector is common to all spectrometers and its figure of merit is the detectivity D^* , given by

$$D^* = (A_d \Delta f)^{\frac{1}{2}} / \text{NEP} \quad (8)$$

where A_d is the detector area in cm², f is the bandwidth in Hz; and NEP is the noise equivalent power, i.e. the radiant flux necessary to give a detector output signal equal to the detector noise. D^* may be considered as the signal-to-noise ratio when one watt of radiation is incident on a detector having a sensitive area of 1 cm² and the noise is measured with an electrical bandwidth of 1 Hz.

The HgCdTe detector selected has a D^* of 6×10^9 cm Hz^{1/2}/W at 1000 cm⁻¹ and an area of 4 mm².

The efficiency η of the optical system varies little for well designed spectrometers. The modulation efficiency for either an interferometer or a chopped system is about 0.35 and the losses due to transmission and reflection in the optics have approximately the same value. In the absence of more exact information, η is usually assumed to be about 0.1.

Two of the terms in equation 5, the throughput θ and the integration time τ , change significantly among spectrometer types.

Jacquinet (28) showed that the interferometric spectrometers (e.g. Fabry-Perot or Michelson) transmitted more radiation to the detector than the dispersion spectrometers of comparable size where a slit was used. This permits simultaneous high spectral resolution and high radiation gathering power. Loewenstein (29) estimates that the throughput θ for the Michelson interferometer is a factor of 200 better than that from a grating spectrometer for equal collimator area and resolving power, all other things being equal.

In communications, many signals can be transmitted through the same channel if they are suitably coded. The technique is called multiplexing, and Fellgett (30) showed that the Michelson interferometer codes each infrared frequency as a cosine wave of low electrical frequency. These electrical frequencies are detected simultaneously and decoded by Fourier analysis. If 300 spectral elements are recorded simultaneously rather than sequentially, and if the noise is from the detector or background photons, full realization of the multiplex gain is possible (31). For a single detector this multiplex gain of a Michelson interferometer is $\sqrt{300}$ over a dispersion instrument.

Hadamard spectroscopy (32), which is still being developed, also achieves this gain advantage using a grating spectrometer with movable masks composed of multiple slits in place of the single slits of the conventional dispersion spectrometer.

On the basis of this analysis we selected a Fourier transform spectrometer, the FTS-14 by Digilab, for the present experiments. The values of the throughput and scan period for this instrument are $\theta = 0.012 \text{ cm}^2 \text{ sr}$ and $\tau = 3.2 \text{ sec}$ at a spectral resolution of 1 cm^{-1} . The components of the throughput θ are $A = 20.3 \text{ cm}^2$ and $\Omega = 6.12 \times 10^{-4} \text{ sr}$. The area corresponds to a nominal aperture diameter of 2 inches and the solid angle is limited by the detector optics. In review, the parameters to be inserted in equation 5 for a Fourier transform spectrometer operating under our experimental constraints are:

$$\begin{aligned}
 \eta &= 0.1 \\
 N_{1000}^b &= 6.18 \times 10^{-6} \text{ W}/(\text{cm}^2 \text{ sr cm}^{-1}) \\
 \Delta\nu &= 1 \text{ cm}^{-1} \\
 \theta &= 0.012 \text{ cm}^2 \text{ sr} \\
 \tau &= 3.2 \text{ sec} \\
 A_d &= 0.04 \text{ cm}^2 \\
 D^* &= 6 \times 10^9 \text{ cm Hz}^{\frac{1}{2}}/\text{W}
 \end{aligned} \tag{9}$$

and the corresponding signal-to-noise ratio is 398.

FOURIER SPECTROSCOPY

The principles of operation of the Fourier transform spectrometer are described in the literature (33, 25, 34) and we will restrict ourselves here to those concepts which are specific to the FTS-14 and which are necessary for an understanding of the techniques of data acquisition and analysis.

An optical diagram of the spectrometer is shown in figure 2. Infrared radiation from a sample enters the Michelson interferometer as shown and is divided by the beamsplitter into two orthogonal components of approximately equal intensity. Each component is reflected from a plane mirror and returned to the beamsplitter for recombination. Part of the recombined radiation then continues to the focusing optics and the infrared detector.

Consider sample radiation which is monochromatic at wavelength λ_0 . If the distances between the beamsplitter and the two mirrors are equal or differ by an even multiple of $\lambda_0/4$, then the two beams recombine constructively and the energy at the detector is a maximum. Conversely, if the optical paths differ by an odd multiple of $\lambda_0/4$, then the energy at the detector is a minimum. The moving mirror M_1 travels at a constant velocity $v = X/T$, where X is the distance travelled by the Mirror M_1 from the position of equal path length and

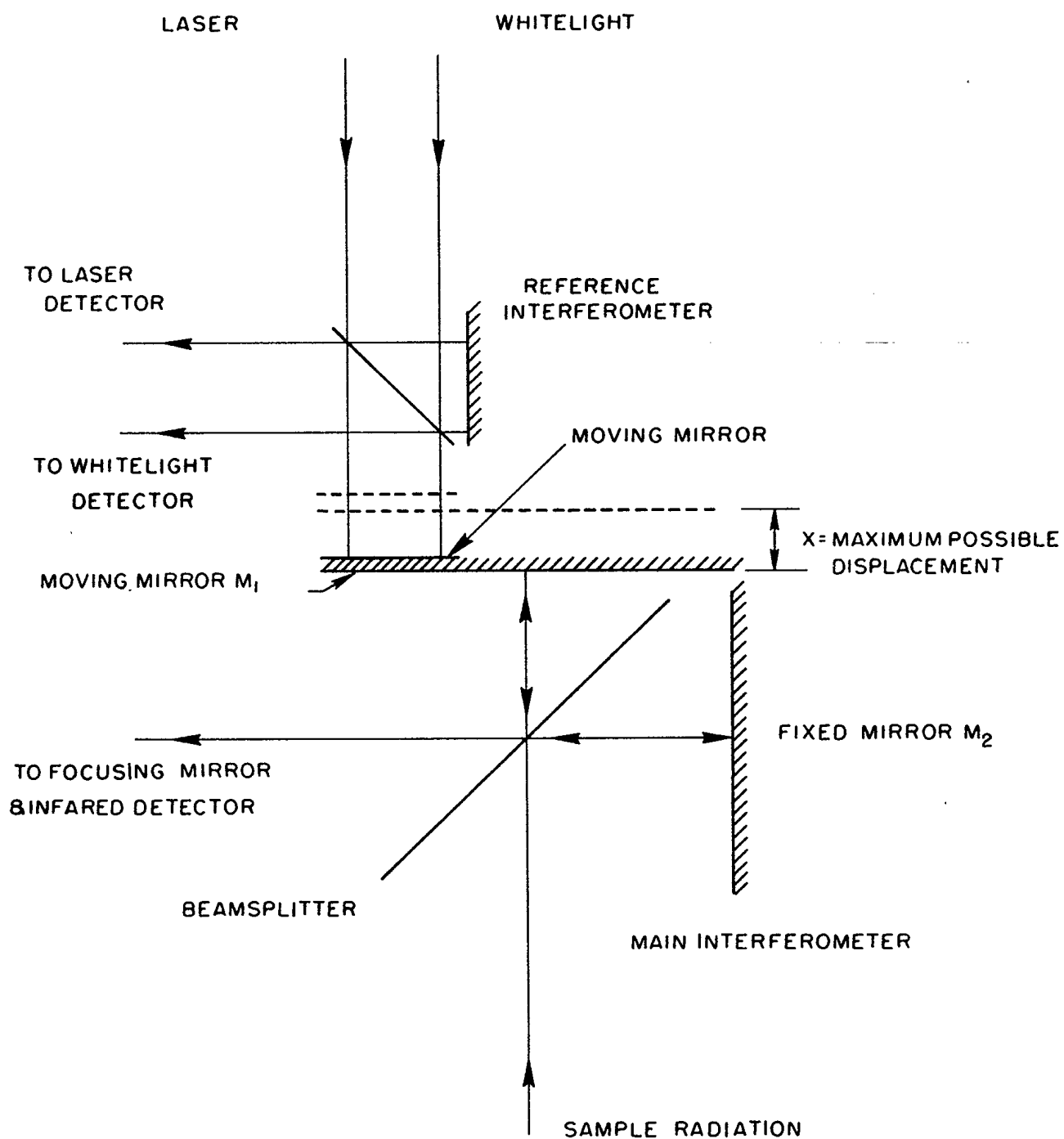


Fig. 2. Optical diagram of the Fourier transform spectrometer.

is one-half of the change in optical path and T is the corresponding scan time. Thus, the signal from the detector is a cosine wave with frequency f_0 given by:

$$f_0 = 2v/\lambda_0 \quad (10)$$

The amplitude of this cosine wave is directly proportional to the intensity of the source radiation at wavelength λ_0 , although the proportionality constant varies with wavelength.

The frequency f_0 is normally in the audio range and when many wavelengths are present in the source radiation, the signal at the detector, called an interferogram, contains the corresponding audio frequencies. At zero displacement of mirror M_1 all components of the interferogram are in phase and generate the characteristic peak shown in figure 4. Hence the Michelson interferometer is a device which translates infrared frequencies to audio frequencies. The audio signal carries all of the information in the infrared beams, but can be detected, amplified, and analyzed using conventional apparatus.

The spectral resolution $\Delta\nu$ is determined by the displacement X during a scan according to (35)

$$\Delta\nu = 1/4X \quad (11)$$

and is independent of spectral region. The solid angle Ω of radiation which can be accepted by the interferometer is also related to the displacement by the relationship.

$$\Omega = \frac{\pi}{2v_{\max} X} \quad (12)$$

If, for example, the source radiation is monochromatic with a wavelength of $10 \mu\text{m}$ (1000 cm^{-1}) and the mirror velocity is 0.156 cm/sec , then the frequency of the electrical signal in the interferogram, from equation 10, is 312 Hz . Similarly, a source radiation of $5 \mu\text{m}$ produces a detector signal of 624 Hz at the same mirror velocity. When the mirror displacement reaches 0.5 cm , the scan time is 3.2 sec and the resolution is 1 cm^{-1} .

The spectrometer moving mirror is mounted on an air bearing and it is driven by an electromechanical transducer similar to that of a loudspeaker. A reference interferometer is placed as shown in figure 2 with its moving mirror back-to-back with the moving mirror of the main interferometer. The reference interferometer operates in the visible with two light sources and two detectors. One source is a He-Ne laser which radiates at $0.6328 \mu\text{m}$. The output of its detector is a cosine wave which generates timing pulses to control the velocity of the moving mirrors and also the sampling of the main interferogram for analog-to-digital conversion. The second source is a white light whose broad band of radiation generates a large peak in the reference interferogram at zero mirror displacement. The position of this peak is adjusted to begin sampling of the main interferogram a short reproducible distance before its position of equal path length.

In the past there has been some confusion over the role of the beamsplitter in the measurement of forward and reverse spectra, i.e. spectra originating on the source and detector sides of the beamsplitter respectively. An understanding of this role is essential for accurate processing of the data because the reverse spectrum is often larger than the forward spectrum when the source is radiating at room temperature or below.

The beamsplitter in the FTS-14 is a thin film of germanium deposited on a potassium bromide substrate. The film reflects radiation from both its surface and the reflected rays reinforce when these surfaces are a quarter wavelength apart (36). The optimum beamsplitter thickness can be obtained for one wavelength only and at longer or shorter wavelengths, the reflectance tends to zero (37). A compensating plate of KBr is mounted a few micrometers away from the germanium surface. The resulting air gap extends the useful bandwidth of the beamsplitter to the spectral region between 2.7 μm and 25 μm (38).

The geometry of the interferometer is shown schematically in figure 3, where the substrate and compensating plate have been omitted for simplicity and the thickness of the germanium film is greatly exaggerated. The moving mirror M_1 is stopped at the position where the two beams of forward radiation have equal path lengths. These two beams recombine constructively for all wavelengths of sample radiation and produce maximum intensity at the detector. The two beams of reverse radiation, on the other hand, differ in path length by two thicknesses of the beamsplitter and therefore recombine destructively to produce minimum intensity at the detector.

When the mirror M_1 is driven at constant velocity, the resulting reverse interferogram looks superficially like the complement of the forward interferogram, which is exactly 180° out of phase with the forward interferogram (38). Figure 4 shows examples of forward and reverse interferograms which were recorded using a fused quartz sample at temperatures of 324.8 K and liquid nitrogen. For the sample at 324.8 K the forward or sample radiation predominates while for the sample at liquid nitrogen temperatures the reverse or spectrometer self-radiation predominates. We do not know the exact phase relationship between forward and reverse interferograms when substrate, compensating plate, and air gap are present, but it should be 180° for some wavelength and should also be wavelength dependent.

Each wavelength component in the forward interferogram adds vectorially to the corresponding component in the reverse interferogram and the resultant may be as much as 180° out of phase with the forward interferogram. It is apparent that the Fourier transform of the resultant interferogram cannot yield a spectrum of the forward radiation without major corrections. Correction is difficult because the phase shifts are large and vary with the intensity of the forward and reverse spectra. Under these circumstances, two options are available: either (a) cool the spectrometer until the reverse spectrum is negligible compared to the forward spectrum, or (b) maintain the reverse spectrum at a constant intensity during a series of measurements and subtract it from the resultant at the interferogram level.

We have chosen the latter option.

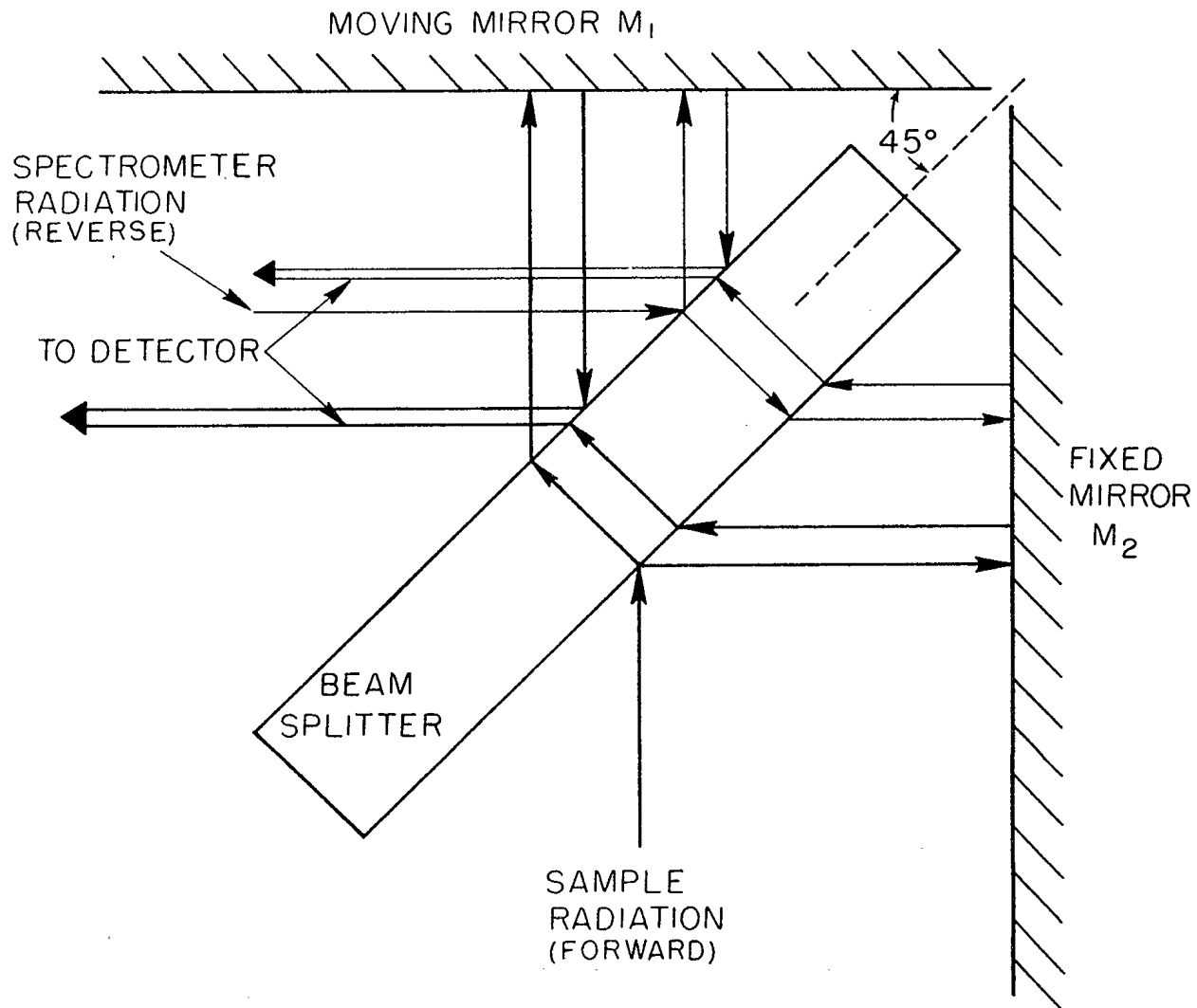


Fig. 3. Beamsplitter operation for forward and reverse radiation.

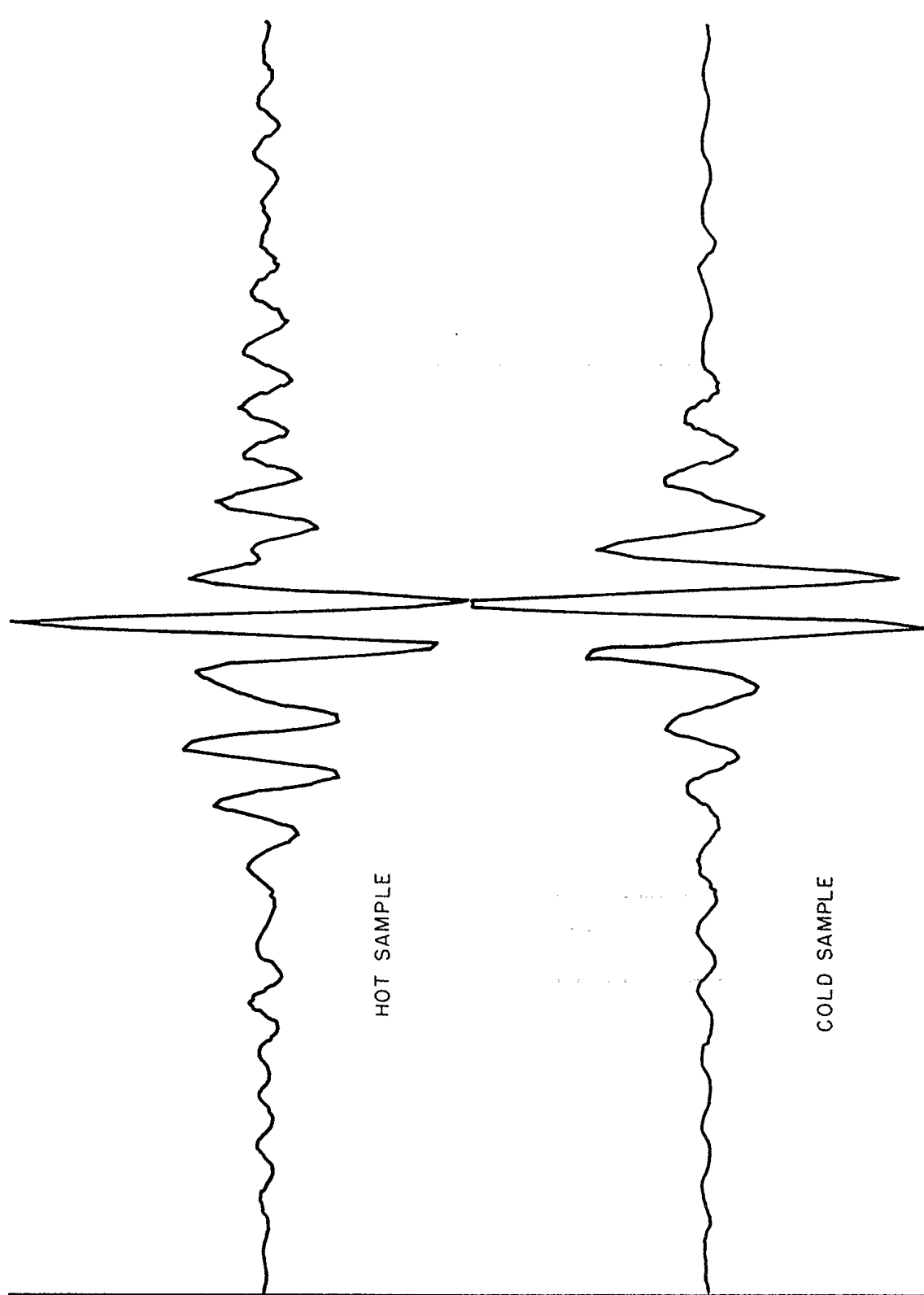


Fig. 4. Interferograms of forward and reverse radiation for a fused quartz sample at temperatures of 77 K and 324.8 K.

MODIFICATIONS TO THE SPECTROMETER

The importance of keeping the reverse interferogram constant led to a few modifications in the spectrometer and its operation. In order to keep the interferometer block at a constant temperature during a series of runs, the room temperature was maintained constant to within 1.0 K, and the head electronics, including the laser, were turned on several hours before measurements were started. The block temperature, which is continuously thermally regulated, was monitored by means of a thermistor to ± 0.01 K.

A Kodak Irtran IV window with antireflection coatings was mounted at the entrance to the spectrometer and a curtain of constant temperature dry nitrogen was used to thermally isolate the window at a fixed temperature. The temperature of the window mount through which the gas flowed for the curtain was maintained constant within ± 0.01 K and close to the interferometer block temperature.

The detector stop probably generates most of the reverse radiation and this stop was provided with a heater, thermoregulator, and thermistor readout.

The air bearing of the interferometer moving mirror was supplied with dry cylinder nitrogen to provide a continuous purge of water vapour and carbon dioxide from the spectrometer to negligible levels.

SAMPLE AND SAMPLE ENVIRONMENT

COLD BOX DESIGN PARAMETERS AND DESIGN CRITERIA

The sample container must provide an environment for the radiating source which will permit accurate measurement of thermal radiation at a known temperature. Before describing in detail the construction of the container and its accessories, those design parameters which are dictated by the environmental needs of the sample and those design criteria which must be met to couple the sample box to the spectrometer will be examined.

The samples to be studied include materials which contain water or other volatile liquids and the radiation characteristics of these materials might be seriously degraded if attempts were made to evacuate the space above the source. It was therefore decided to fill the sample box with a transparent gas such as nitrogen to a pressure slightly above atmospheric. The presence of the gas means that the energy interchange at the sample surface will take place by convection as well as by radiation and conduction.

The definition of emissivity in equation 1 shows that we must measure the thermal radiation from the sample and divide it by the corresponding radiation from a blackbody at the same temperature. Two practical problems arise when we

try to make these measurements. First, if the sample is close to ambient temperature and is surrounded by objects which are at ambient temperature, then the surface under test is bathed in infrared radiation of about the same intensity as that being emitted. Equation 4, derived from Kirchoff's law, shows that there is no information available about emissivity in the extreme case where the environment is at the same temperature as the sample. In this case the sum of reflected and emitted radiation is just equal to the blackbody radiation at that temperature and so the apparent emissivity is one. When the reflected component is made much greater than the emitted component then emissivity may be inferred from measured reflectivity using equation 4. This was the only way to obtain emissivity at ambient temperature before sensitive spectrometers were developed.

The sample surface can be shielded from most of the stray radiation by a cold black collimator. The two most convenient temperatures for this cold shield are those of solid carbon dioxide (193 K) and liquid nitrogen (77 K). Figure 5 shows that the radiation from a black surface at 193 K is too large compared to that from a black sample at 273 K and therefore the lower temperature of liquid nitrogen was chosen.

There is a net loss of radiation from the sample surface to the cold shield and the flow of nitrogen gas also transports heat from the sample to the shield. This cooling of the sample surface introduces the second problem in measuring emissivity - uncertainty in the temperature of the radiating surface. A temperature gradient develops through the sample and the very thin radiating surface is no longer at substrate temperature. An accurate correction for this temperature gradient can seldom be made because neither the energy exchange at the surface nor the thermal conductivity of the sample material is known with sufficient precision. An error of 0.5 K in the determination of the surface temperature of the sample at 273 K means an error of almost 1% in the measured value of emissivity at peak radiance and this error increases with decreasing wavelength.

There are several ways to replace the energy lost by radiation and convection. Heat may be supplied by conduction from a substrate, by radiation at a wavelength outside the spectral region of interest or by (convection from) a curtain of warm gas. The non-equilibrium technique of alternately soaking the sample in an oven at the desired temperature and exposing it briefly to the spectrometer is used at higher temperatures (39) but was not considered suitable for the sometimes fragile samples which were anticipated here.

In the natural night environment the loss of energy from the surface of the earth by radiation to cold space is replenished chiefly by natural convection from the atmosphere and heat conduction from below.

In view of the above requirements it was decided in our experiment to supply heat to the sample surface by conduction from a thermally regulated substrate and by forced convection of a curtain of thermally regulated dry nitrogen above it. The equilibrium temperature from radiation and convection above is first measured at the surface of an insulated black source of known emissivity. Then the substrate of the material being studied is maintained at this equilibrium temperature to eliminate gradients through the sample. In this way a surface temperature can be confidently assigned to the surface even though the heat conductivity through the material is small or unknown.

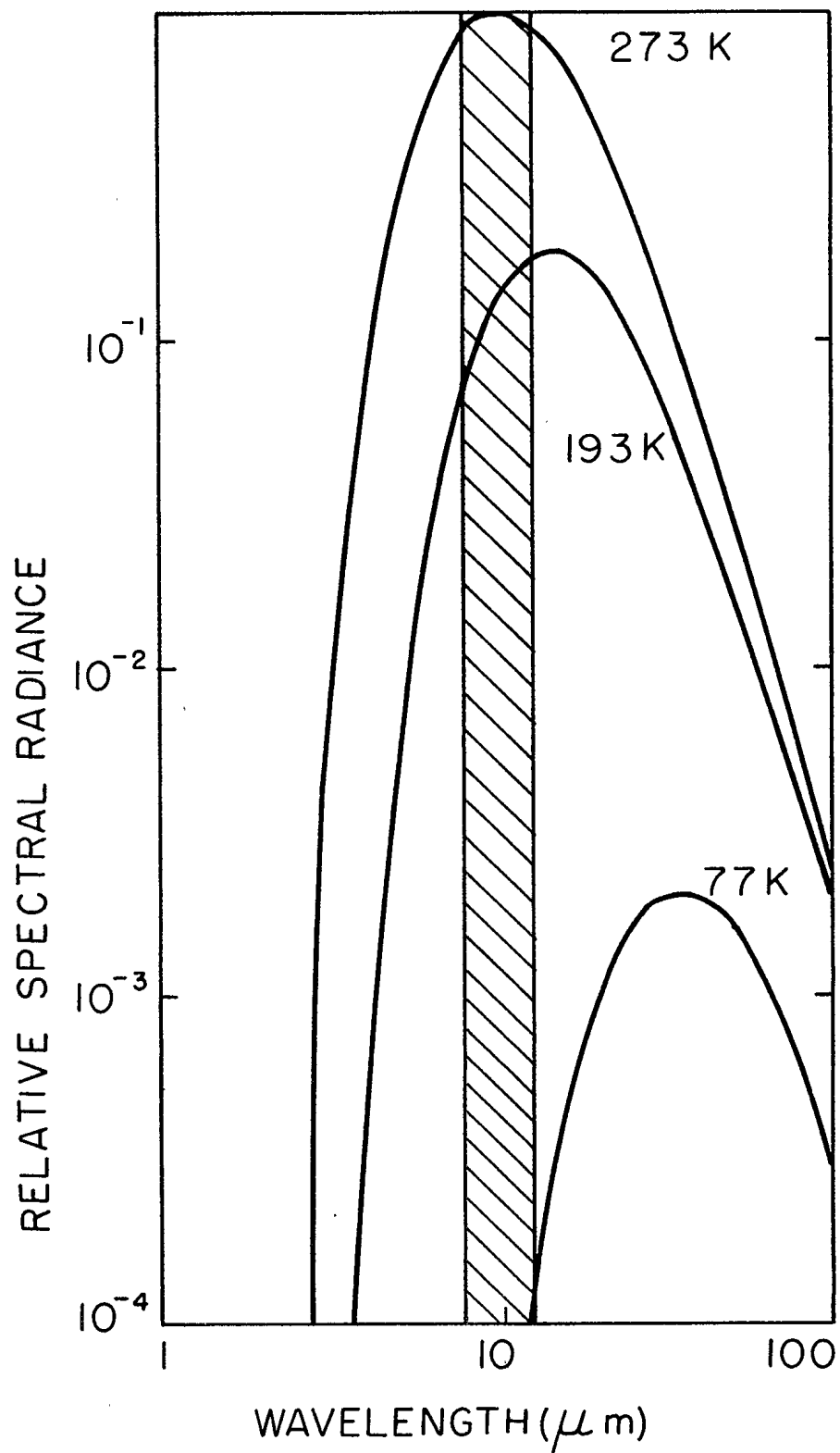


Fig. 5. Relative spectral radiance from blackbodies at 273 K, 193 K (dry ice), and 77 K (liquid nitrogen).

The use of a gas curtain to warm the top of the sample means that this surface is exposed to radiation from the gas nozzle as well as from the spectrometer and its window. This radiation is not negligible and the component reflected from the sample surface into the spectrometer must be subtracted from the sample radiation to obtain the portion due to thermal emission above. The reflected component can be separated by cooling the sample while maintaining the radiation incident on the sample surface. In many cases the sample may be cooled to liquid nitrogen temperature to reduce thermal emission to a negligible level. Then the measured spectrum, corrected for instrumental background, can be assigned to the reflected component alone.

SAMPLE - INSTRUMENT INTERFACE

The surface of the moving mirror in the Michelson interferometer is vertical because the air bearing of the driving motor should be horizontal. In addition, the sample surface must be horizontal because liquids and aggregates will be studied. The sample box was therefore designed with a front surface folding mirror at 45 degrees to direct sample radiation into the spectrometer.

The entrance aperture of the spectrometer is limited mainly by the beamsplitter mount and is irregular in shape but approximates an ellipse with horizontal and vertical axis of 1.63 inches and 2.25 inches respectively. The half angle field of view is limited by a stop in the detector optics to about 0.7 degrees. In order to fill most of the field of view, the sample surface was stopped down to a diameter of 2 inches by an aperture in the radiation shield although the actual sample diameter was extended to 2.5 inches to reduce edge effects.

Since the exposed sample surface does not completely fill the field of view of the spectrometer, it is necessary to maintain the alignment between box and spectrometer during a series of runs. Therefore the base of the cold box was rigidly attached to the base of the spectrometer.

COLD BOX CONSTRUCTION

A schematic cross section of the box is shown in figure 6. The baseplate of half-inch aluminum, thermally regulated to room temperature, was bolted to the spectrometer through insulators. The view box on top of the baseplate held the front surface folding mirror on hinges so it could be moved out of the way to inspect the sample surface. The mirror stop at 45° and the viewbox on the baseplate were adjustable so radiation from the source could be directed axially into the spectrometer. A flexible tube joined the viewbox to the frame for the spectrometer window to reduce the loss of nitrogen gas from the weakly pressurized box.

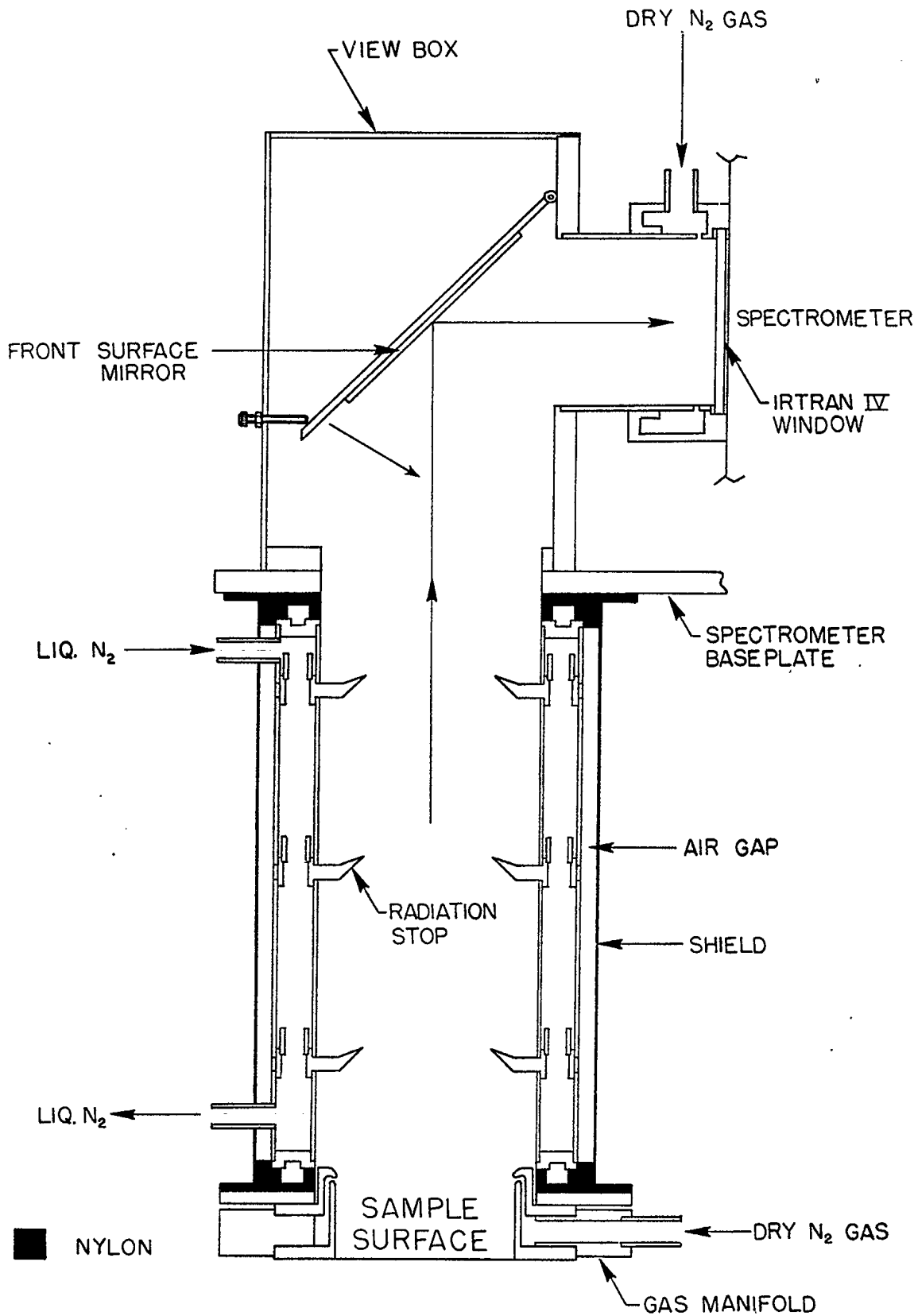


Fig. 6. A schematic cross section of the cold box.

The radiation shield was suspended from the baseplate, as shown in Figure 6, and was insulated at the top and bottom by nylon spacers. Aluminum was used for the shield itself and the parts were held together with silicone rubber. Three cold apertures limited the stray radiation to the sample and defined the part of the sample surface which could radiate to the spectrometer. The lower aperture is shown in more detail in Figure 7. Liquid nitrogen was pumped into the hollow shield wall at the top and percolated through three trays to the bottom where it drained out of the box to an overflow detector. Nitrogen gas, which was pumped into the sample box above the sample and at the window, left through exhaust ports (not shown) near the middle of the radiation shield. The inside of the shield, including the apertures, was sandblasted and painted with Krylon 1602 ultra-flat black paint. This paint was chosen because of its emissivity varied from 0.98 to 0.99 over the 8 to 13 μm wavelength region (40).

A thermocouple junction was buried in the top aperture about 1/8 inch from the edge to monitor the temperature. The leads of the thermocouple were insulated with styrofoam but conducted some heat to the junction which resulted in temperature readings which were too high. A temperature of 99 K was recorded five minutes after activating the liquid nitrogen pump and the temperature rose to 111 K three minutes after the pump was stopped. The lowest temperature recorded was 83 K.

The radiation shield remained free of frost except occasionally after samples were changed or when wet samples were mounted. A grey colour near the inner edge of the aperture stops showed that sublimation had taken place. However frost has an emissivity as large as black paint in the 8 to 13 μm band and hence a thin deposit does not change significantly the emission from the shield.

The construction of the gas manifold and the sample mount is shown in more detail in Figure 7. The aluminum manifold was polished to reduce infrared emission and thermally regulated to control the temperature of the nitrogen curtain. The manifold temperature was monitored at the nozzle with a thermistor thermometer.

All radiation sources were cylindrical with an outside diameter of 2.5 inches to fit inside interchangeable mounting flanges which consisted of an insulating nylon sleeve and an aluminum mounting ring. The ring was attached to the bottom of the gas manifold with quick release bolts. The construction and use of several types of radiation source is described below. Two of these sources are illustrated schematically in Figure 8.

RADIATION SOURCES

THE BLACKBODY SOURCE

The blackbody source was a 10 inch length of aluminum tubing with a 1/8 inch wall which was internally sandblasted and painted with Krylon 1602 ultra-flat black paint. The 1/4 inch thick aluminum disk which formed the

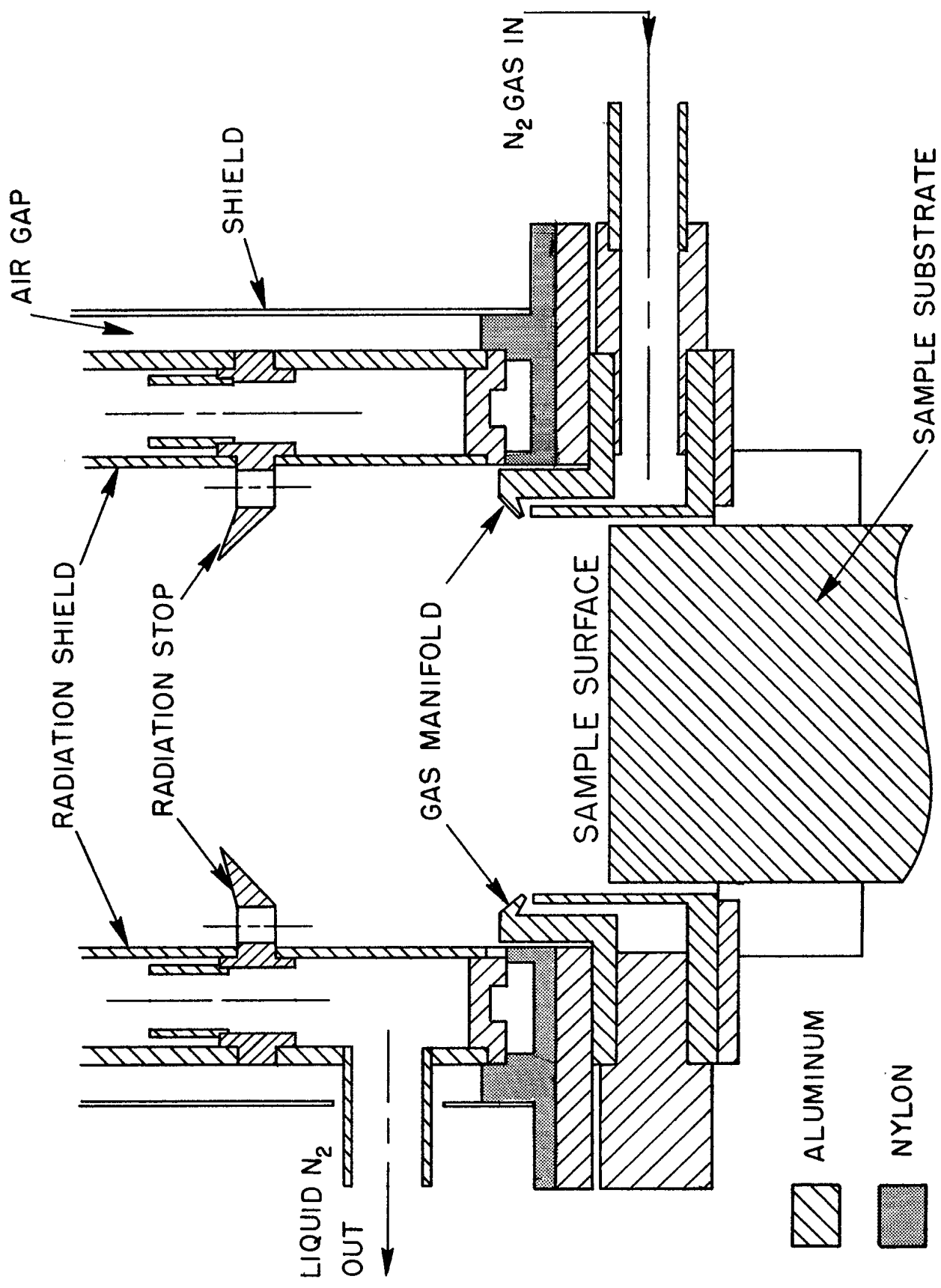


Fig. 7. Details of cold box showing sample gas manifold.

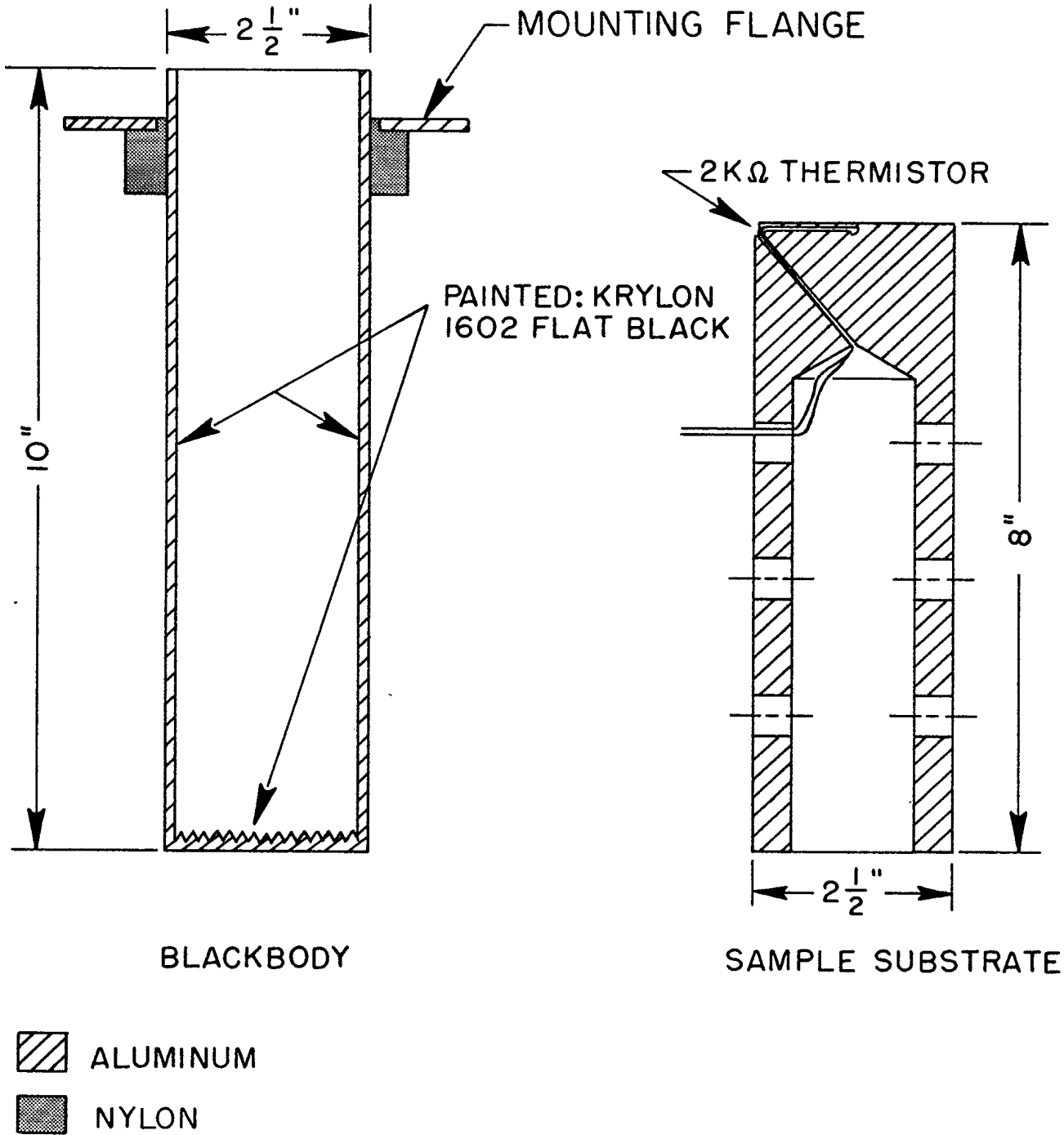


Fig. 8. Blackbody source and sample substrate.

bottom of the source was machined with contiguous 60° annular grooves, about 1/8 inch deep, to reduce reflections. The disk was also painted flat black and sealed to the tube with silicone rubber. This source was immersed in a dewar of liquid nitrogen to produce an extremely low temperature blackbody source or in a dewar containing other thermally-controlled bath liquids to generate blackbody spectra at temperatures up to 373 K. This constant temperature bath was made by mounting a 320 watt heater and a nitrogen bubbler of sintered glass at the bottom of a two liter cylindrical dewar. Thermistors for the thermoregulator and the temperature readout were mounted about half-way down the inside of the dewar. Water was used as the bath for temperatures above 273 K and ethylene glycol and water for temperatures immediately below 273 K. The gas bubbler was used with distilled water and ice to obtain a uniform temperature of 273 K.

INSULATED BLACK SOURCE

The insulated black source was made by gluing a sheet of paper to the end of a styrofoam cylinder and painting the paper with Krylon 1602 ultra-flat black paint. The surface temperature of this source was determined by the flow of warm nitrogen gas from the manifold jet as it mixed with cold gas in the cold box and, to a smaller degree, by radiation into the cold background. Heat conductivity through the styrofoam was negligible and the equilibrium temperature was reached quickly. This source was used to measure, by means of its radiated spectrum, the effective surface temperature.

A source of this type was also used to optimize the shape of the manifold nozzle. When pre-cooled and frost-covered, this source demonstrated non-uniform heating by preferential melting and evaporation, as observed through the window of the viewing box.

The insulated black source was also used to monitor the change in equilibrium radiation temperature when the manifold temperature, gas flow rate, and height of the gas nozzle above the sample surface were changed. It was found that the surface temperature was not very sensitive to the gas flow rate or temperature but that the position of the sample surface had to be maintained within 0.25 mm in order to ensure that equilibrium radiation temperature was reproducible within 0.5 K.

SAMPLE SUBSTRATE

The sample substrate was a solid aluminum cylinder, 10 inches long, with holes machined in the lower part to increase contact with the bath liquids. A calibrated thermistor was inserted in a hole 1/8 inch below and parallel to the radiating surface. The temperature of the surface was controlled by the constant temperature bath, but measured by the calibrated thermistor.

A black source was made using this substrate by painting the radiating surface with Krylon 1602 ultra-flat black paint. This source was used to measure the temperature of the insulated black source by spectral matching and to measure emissivity of the black paint by dividing its spectrum by that of a blackbody source.

Other sample sources were made by placing the sample material upon the substrate.

A low wall around the top of the cylinder contained liquids and fine aggregates. Other materials, particularly those in sheet form, were simply glued temporarily to the end of the cylinder.

ALIGNMENT SOURCE

A He-Ne laser was mounted so its beam coincided with the axis of the cold box. The beam intensity was reduced to a safe level with a disk of exposed film. This source was used to align the cold box axis to the spectrometer axis. The alignment procedure (with spectrometer beamsplitter and window removed) consisted of adjustments to the folding mirror (two degrees of freedom) and to the cold box base with respect to the spectrometer until the laser beam was reflected back on itself from the centre of the main interferometer moving mirror. A white target surrounded the laser beam port so that the reflected beam could be easily seen when it was not coincident with the outgoing beam.

REFLECTING SOURCE

A disk of aluminized plate glass was mounted with three external adjusting screws so that the reflecting surface could be positioned normal to the cold box axis. The criterion for correct alignment was a minimum signal from the spectrometer detector. This source was used to reflect radiation from the spectrometer back into the spectrometer so that its spectrum could be measured.

COLD BOX ACCESSORIES

NITROGEN GAS GENERATOR

To purge the interior of the cold box dry nitrogen gas was generated by boiling liquid nitrogen from a 30 liter dewar. It was found that cylinder nitrogen (prepurified) contained water vapour which condensed on the inside of

the cold box. A 450 watt electric heater at the bottom of the dewar produced gas at the rate of 230 standard cubic feet per hour (SCFH) when supplied with 110 V ac. This flow rate was sufficient to supply the window and sample gas manifolds. A smaller flow rate of about 60 SCFH kept the cold box free of condensation during standby or while the cold box was warming to room temperature.

The cold dry nitrogen from the generator was warmed in a heat exchanger which formed a turret on top of the dewar. A 1300 watt electric heater in the heat exchanger was regulated to keep the gas at room temperature ± 5 K. A thermistor mounted on the 450 watt gas generator heater triggered an alarm and turned off the electric power when the liquid nitrogen in the dewar was almost exhausted. Consumption of liquid nitrogen was about 10 liters per hour.

LIQUID NITROGEN PUMP

A centrifugal pump (41) was mounted at the bottom of a 30 liter dewar and driven through an insulating shaft by a motor mounted in a turret on top of the dewar. This turret could be pressurized and was kept at room temperature by a regulated heater. A filling port allowed the dewar to be recharged with liquid nitrogen without removing the pump or motor. The liquid nitrogen conduit from the pump passed through an insulated seal in the turret and part of the nitrogen gas which was generated in the cold box was fed back into the dewar via the sealed turret to equalize the pressure on the pump.

The pump could supply liquid nitrogen faster than it was needed at the cold box and two controls limited the flow. The pump motor was cycled on and off by a timer with cam controlled microswitches. The period of this cycle was three seconds and the 'on' part was normally about one second.

When the cold box trays were filled with liquid nitrogen the excess overflowed to a thermistor in a heated cavity. This thermistor, when cooled, parked the timer in the 'off' position until the heated cavity evaporated its charge of liquid nitrogen. The warmed thermistor then restarted the pumping cycle.

The pump was switched off during scanning to prevent mechanical vibration and electrical interference at the spectrometer. When the total scan time exceeded the liquid boil-off the spectrometer scans were stopped temporarily while the cold box was refilled. In this case a manual override switch operated the pump continuously for rapid refilling. Liquid nitrogen consumption was usually about 15 liters per hour.

SPECTROMETER SOFTWARE

GENERAL DESCRIPTION OF COMPUTER AND PERIPHERALS

The operation of the Fourier transform spectrometer is controlled through a Nova 1200 mini-computer which presently has 12 K of core storage although operation with as little as 4 K is possible. In either configuration some form of auxiliary storage is needed. In our case this auxiliary storage consists of a 128 K fixed head disk and an Ampex TMZ magnetic tape unit. The disk is used to store the operating system and collected data while the magnetic tape is used to provide a system back-up, store utility programs which are not used frequently, store collected data, and store a disk operating system which is used in the development of further software. All communication to and from the computer is via an ASR-33 teletype which is capable of character transmission speeds up to 10 characters per second. Spectrometer-computer communication is via 16 bidirectional lines. Also interfaced to a Nova is a Houston Instrument DP-1 incremental plotter which is used to display data in graphical form.

Analog data from the spectrometer is converted to digital form by a 15-bit A/D, sample and hold, converter. This converter has a sampling rate of 7000 Hz, a digitization time of 120 ms and the option of being multiplexed to several input analog devices. Data from the converter may enter the computer core either under program control at rates in excess of 10 kHz or through the direct memory access data channel at rates in excess of 200 kHz. Since input through the data channel may be added to an existing number in core, coherent addition of the interferograms of a number of spectrometer scans is possible.

The FTS software operating system controls the collection of data according to the parameters set by the operator. This system is stored on disk in the first 128 sectors and the appropriate portions are called to core by an executive program as the need arises.

It is possible to collect data at a resolution of 0.5, 1, 2, 4, 8 and 16 wavenumbers (cm^{-1}). The number of times that the interferogram must be sampled is dependent on the resolution, ranging from 16384 times at a resolution of 0.5 cm^{-1} to 1024 at 8 cm^{-1} . This sampling rate is determined by the Nyquist sampling theorem which states that the sampling rate must be at least twice the highest frequency present in the record in order not to lose data (42). The operating system determines automatically, for a given resolution, the sampling rate according to the above theorem but the operator may override this feature and specify any other sampling rate.

The collected data is stored on disk in files and referenced by file numbers. Table 1 shows the relationship between resolution and file size. The discrepancy between the maximum possible number of files and the actual number of available files arises because part of the upper portion of the disk is reserved for the storage of utility programs.

The collection and/or analysis of data is carried out by computer upon receipt of a command list. This list is supplied to the computer via the teletype and may consist of a single command or a series of commands up to a

T A B L E I

Relationship Between Resolution and Disk File Space

RESOLUTION	16	8	4	2	1	0.5
Number of data points per file	1024	1024	2048	4096	8192	16384
Number of sectors per file	4	4	8	16	32	64
Maximum number of storage files on disk	95	95	47	23	11	5
Actual number of storage files available	87	87	43	21	10	4

maximum of 15. Included in this command list may be a reassignment of control parameters. That is, the control parameters may be up-dated on the fly. The maximum number of up-dates in any command list is 63.

THE FTS-14 OPERATING SYSTEM

Consider now some of the details of the FTS-14 operating system.

SCAN ADDITION

It is possible to add coherently a large number of scans and hence obtain a good signal-to-noise ratio. The maximum number of scans is 32,000 but in practice this upper limit is never reached due to time considerations and the restrictions on the magnitude of the collected numbers. When a storage area reaches a percentage of the maximum possible value (this percentage is set by the operator) an impending overflow message is sent to the teletype and the spectrometer scanning is terminated. This maximum value of a storage area is $2^7(x)$ where $0 \leq x \leq 32767$.

FOURIER TRANSFORMATION

After the data is collected as an interferogram it may be stored on disk and/or a power spectrum may be calculated using the fast Fourier transform technique of Cooley and Tukey (43). This algorithm has been instrumental in making data analysis of interferometric data using computers feasible since it has reduced the number of terms which must be calculated from N^2 to $N \log_2 N$ where N = the number of digitized points. This has resulted in savings in computing time of as great as 4 orders of magnitude (44), although some of this time saving can be attributed to the development of faster computers.

APODIZATION FUNCTION

Because data is collected only over a finite time interval there is a built-in box-car apodization of the collected data. This apodization affects the data analysis since the computer spectrum is a convolution of the true power spectrum and the Fourier transform of the apodization function. Such a box-car function does not degrade the resolution but its Fourier transform has

non-negligible modulations about a central maximum which can distort small spectral features. In order to counter this, the software system allows us to change the apodization function to a triangular function or to some trapezoidal-shaped function which has properties intermediate to those of the box-car and triangular functions.

The effect of using a triangular apodization function is a reduction of the distortion of small spectral features at the expense of a reduction of the resolution by a factor of two.

PHASE AND COMPENSATION ERRORS

Phase and compensation errors may produce an asymmetric interferogram and hence modify the observed emission spectra. Such errors may result from a digitization procedure which does not digitize exactly at the central maximum of the analog signal from the spectrometer and from imperfections in the spectrometer optics system respectively. These errors may be corrected by collecting the interferogram over both positive and negative values of the path difference and calculating both the sine and cosine transforms. This, however, would necessitate the collection of twice as many data points and also would raise the noise level because the procedure involves a squaring to give the amplitude of the spectra and hence changes the noise from a function fluctuating randomly about zero to one fluctuating about some positive value. If, however, this phase correction is small, which is usually the case, a correction may be made by calculating a phase function from the sine and cosine transforms for a small number of data points on either side of the central maximum. The number of points used in this calculation is set by the operator to any positive integer from 2 to the number of points between the white light peak of the interferogram. The calculation of this phase correction may however be suppressed. In this case the phase array which was stored from the last computation is used to compute the power spectrum.

FILE SUBTRACTION

It is possible to subtract two files point-by-point. This may be done at either the interferogram or power spectrum level. With the present software there is no check for overflow upon subtraction and consequently the subtraction of a large positive number from a large negative value or vice versa will result in an incorrect value if overflow occurs. The software, in such a case, replaces the actual result with the largest positive or negative number it can accommodate, according to whether the actual result should be positive or negative. The effect that such errors in an interferogram may cause in the power spectrum is illustrated by Horlick and Malmstadt (45). In order that such an error does not occur we scale down both files by a factor of two before subtraction.

PLOTTING DATA

The collected data may be plotted either as an interferogram or a power spectrum. The operator may choose:

- a) the abscissa and ordinate scales
- b) the mode of the power spectrum plot
- c) the wavelength interval of the power spectrum plot
- d) a smoothing procedure

The process of plotting the data, in any mode, does not change the stored data. Hence the same piece of data may be plotted several times with different plot parameters. The power spectrum may be plotted as an emission spectrum, a transmission spectrum, or two forms of absorption spectra. Both the transmission and absorption plots are ratios of the actual spectrum to some reference spectrum. In the transmission mode the ordinate is linear in percent of transmission while in the absorption mode the ordinate may be either linear or logarithmic in absorption.

It is also possible to introduce a smoothing factor into the plot which has the effect of trading resolution for signal-to-noise ratio. As in the other cases the spectral data in disk storage is not disturbed and may be replotted in its original form at another time.

ALARM SIGNALS

The software operating system also monitors the spectrometer for any abnormalities and alerts the operator to the situation by outputting a message to the teletype. Examples of the alarm signals are:

- 1) low air pressure: the pressure in the air bearing has dropped below 30 psi.
- 2) laser off: the laser is either non-functional or its output is below the required intensity level.
- 3) non-Digilab position: the switches on the spectrometer instrument panel are not in the correct positions for computer control.
- 4) align position: the spectrometer alignment is misadjusted.
- 5) A/D overflow: a signal greater than 15 bits has been measured by the A/D converter.
- 6) impending overflow: a word is about to become greater than the value set to signify overflow.

DATA ACQUISITION

EMISSIVITY CALCULATIONS

GENERAL FORM OF EMISSIVITY EQUATION

In general the input radiation to the spectrometer detector is the sum of background radiation and radiation emitted by and reflected from the sample. Mathematically this radiation may be characterized as

$$\vec{S}_\lambda(T_S) = K_\lambda \left\{ \epsilon_\lambda \vec{N}_\lambda^b(T_S) + \vec{R}_\lambda + \vec{W}_\lambda \right\} \quad (13)$$

where $\vec{S}_\lambda(T_S)$ = the radiation, which is wavelength λ dependent, impinging on the spectrometer detector when a sample, at temperature T_S , fills the field of view of the instrument

K_λ = the instrument profile

ϵ_λ = the emissivity of the sample

$\vec{N}_\lambda^b(T_S)$ = the radiation from a blackbody at temperature T_S

\vec{R}_λ = the radiation reflected from the sample

and \vec{W}_λ = the background radiation

The vector notation is introduced to emphasize the fact that the relative phase of the various terms on the right side (RHS) of this equation must be taken into account in the subsequent data analysis. Consider now the various terms in equation 13.

The radiation emitted by the sample, $\epsilon_\lambda \vec{N}_\lambda^b(T_S)$, is characterized by the product of its emissivity and a term describing the radiation from a blackbody at the sample temperature T_S . This radiation is a function of the molecular and crystalline structure of the material and the surface properties of the sample.

If a sample has an emissivity less than 1.0 it follows from equation 4 that it will possess a finite reflectance and hence a portion of the radiation incident upon its surface will be reflected into the field of view of the spectrometer. Because of the cold box design the reflected radiation \vec{R}_λ

originates mainly from the manifold and the spectrometer. Since the manifold is kept at a constant temperature, in the range from 303 to 323 K throughout a series of runs, the contribution to the reflected radiation from the manifold will remain constant. Furthermore the radiation from the spectrometer originates at the detector stop, the beamsplitter, the spectrometer head, and the Irtran IV window all of which are maintained at a fixed temperature or in a stable thermal environment. Consequently the total incident radiation upon, and hence reflected from the sample remains constant and varies from sample to sample only due to the different reflectivities of their surfaces. Also the background radiation

\vec{W}_λ which results primarily from the spectrometer, is a constant quantity since the spectrometer assembly is maintained in a stable thermal state. In actual fact our sample holder does not fill the field of view of the spectrometer and the lower aperture stop of the cold box, which is maintained at near liquid nitrogen temperatures, is partly within the field of view but it emits a negligible amount of radiation.

Finally, the measured signal is modified by the response function of the system which is a manifestation of the detector spectral response function and any imperfections or peculiarities in the optical components along the path the input radiation follows through the spectrometer.

PARAMETERS REQUIRED TO SOLVE THE EMISSIVITY EQUATION

Equation 13 involves four unknowns, namely ϵ_λ , \vec{W}_λ , \vec{R}_λ , and K_λ and subsequently four independent equations involving the unknowns are required in order to solve for any of these quantities. These additional equations are obtained from the following three measurements:

(a) By recording the radiation $\vec{S}_\lambda(T_Q)$ from the sample at some temperature T_Q

$$\vec{S}_\lambda(T_Q) = K_\lambda \left\{ \epsilon_\lambda \vec{N}_\lambda^b(T_Q) + \vec{R}_\lambda + \vec{W}_\lambda \right\} \quad (14)$$

(b) By recording the radiation $\vec{B}_\lambda(T_B)$ from a blackbody at temperature T_B

$$\vec{B}_\lambda(T_B) = K_\lambda \left\{ \vec{N}_\lambda^b(T_B) + \vec{W}_\lambda \right\} \quad (15)$$

(c) By recording the radiation $\vec{B}_\lambda(T_L)$ from a blackbody at temperature T_L

$$\vec{B}_\lambda(T_L) = K_\lambda \left\{ \vec{N}_\lambda^b(T_L) + \vec{W}_\lambda \right\} \quad (16)$$

In practice T_L is chosen to be the boiling point of nitrogen which is attained by immersing the blackbody sample into a dewar of liquid nitrogen. Consequently the term $|\vec{N}_\lambda^b(T_L)|$ becomes negligible compared to $|\vec{W}_\lambda|$ and hence equation 16 becomes

$$\vec{B}_\lambda(T_L) = K_\lambda |\vec{W}_\lambda| \quad (17)$$

or just a measure of the background radiation modified by the response function of the spectrometer.

Likewise in practice the temperature T_Q of the insulating sample is chosen to be the temperature of liquid nitrogen and in this case $|\epsilon_\lambda \vec{N}_\lambda^b(T_Q)|$ becomes negligible with respect to $|\vec{R}_\lambda|$ and $|\vec{W}_\lambda|$. However for this discussion the term $\epsilon_\lambda \vec{N}_\lambda^b(T_Q)$ will be retained in order to illustrate the general result.

SOLUTION OF EMISSIVITY EQUATION

Now since \vec{R}_λ and \vec{W}_λ are constant quantities, they may be eliminated from the equations by subtracting equation 14 from 13 and 17 from 15 to yield

$$\vec{S}_\lambda(T_S) - \vec{S}_\lambda(T_Q) = K_\lambda \left[\epsilon_\lambda \vec{N}_\lambda^b(T_S) - \epsilon_\lambda \vec{N}_\lambda^b(T_Q) \right] \quad (18)$$

and

$$\vec{B}_\lambda(T_B) - \vec{B}_\lambda(T_L) = K_\lambda \left[\vec{N}_\lambda^b(T_B) \right] \quad (19)$$

The subtraction on the LHS is carried out at the interferogram level and then the Fourier transform is applied to the subtracted result to produce a power spectrum. This procedure is followed in order to account for the phase relationship between the various terms in equations 13 to 17. Performing the Fourier transform before the subtraction would destroy this phase information. It was shown earlier that the interferogram of the self-radiation from the spectrometer, which traverses the spectrometer in the reverse direction, is approximately 180° out of phase from the radiation which traverses the spectrometer in the forward direction. For our calculation procedure to be valid, it is not necessary that we know the phase relationship between the various terms of equation 13, only that this relationship does not change throughout the experiment. Because of this importance of the phase relationship, all data which is kept for future reference is stored as an interferogram.

Returning now to equations 18 and 19, the vector notation is dropped once the subtraction and Fourier transform operations are applied to the LHS of these equations. The vector notation on the RHS is dropped because all the terms on this side are forward blackbody radiation terms and hence in phase. Thus these equations become:

$$\left| \vec{S}_\lambda(T_S) - \vec{S}_\lambda(T_Q) \right| = K_\lambda \left[\epsilon_\lambda \left| \vec{N}_\lambda^b(T_S) \right| - \epsilon_\lambda \left| \vec{N}_\lambda^b(T_Q) \right| \right] \quad (20)$$

and

$$\left| \vec{B}_\lambda(T_B) - \vec{B}_\lambda(T_L) \right| = K_\lambda \left| \vec{N}_\lambda^b(T_B) \right| \quad (21)$$

Thus from these two equations the profile term may be removed by dividing one by the other and hence the emissivity becomes:

$$\epsilon_\lambda = \left\{ \frac{\left| \vec{S}_\lambda(T_S) - \vec{S}_\lambda(T_Q) \right|}{\left| \vec{B}_\lambda(T_B) - \vec{B}_\lambda(T_L) \right|} \right\} \left\{ \frac{\left| \vec{N}_\lambda^b(T_B) \right|}{\left| \vec{N}_\lambda^b(T_S) - \vec{N}_\lambda^b(T_Q) \right|} \right\} \quad (22)$$

These calculations take into account the reflectance of spectrometer and manifold radiation from the sample. To show that this is necessary consider the magnitude of the reflectance term $\left| \vec{R}_\lambda \right|$ in equation 13. From equations 14, 15, and 17 with T_Q at liquid nitrogen temperature

$$\frac{|\vec{R}_\lambda|}{|\vec{N}_\lambda^b(T_B)|} = \frac{|\vec{S}_\lambda(T_Q) - \vec{B}_\lambda(T_L)|}{|\vec{B}_\lambda(T_B) - \vec{B}_\lambda(T_L)|} \quad (23)$$

Figure 9 shows a plot of this ratio for a fused quartz sample to a blackbody at a temperature T_B of 273 K. It can be seen that this term is small compared to the emission from a blackbody at ambient temperature but not negligible.

Consider equation 22 again. In practice T_S and T_B were chosen to be close to 273 K. With this choice it is necessary to have $|T_S - T_Q|$ greater than about 40 K otherwise a small error in the determination of either of these temperatures will result in an unacceptable error in the quantity $|\vec{N}_\lambda^b(T_S) - \vec{N}_\lambda^b(T_Q)|$. For example assuming that T_S was measured correctly but T_Q was in error by 0.5 K (for $T_S = 273$ K and $|T_S - T_Q| = 40$ K), the error in $|\vec{N}_\lambda^b(T_Q)|$ is 1.5% for $\lambda = 10 \mu\text{m}$. In practice, for insulating samples, T_Q was chosen to be at liquid nitrogen temperature by placing the sample holder in a dewar of liquid nitrogen. In order to reduce the sample surface temperature to this value it is necessary to shut off the gas flow from the manifold to the sample surface. However, the rate of flow of dry nitrogen through the cold box should be maintained at a constant value otherwise the temperature of the Intran IV window between the cold box and spectrometer can change and hence the background radiation. Consequently when the flow of nitrogen is shut off from the manifold it is redirected into the cold box assembly at the viewing box.

Hence by choosing T_Q to be the boiling point of liquid nitrogen equation 22 becomes

$$\epsilon_\lambda = \left\{ \frac{|\vec{S}_\lambda(T_S) - \vec{S}_\lambda(T_Q)|}{|\vec{B}_\lambda(T_B) - \vec{B}_\lambda(T_L)|} \right\} \left\{ \frac{|\vec{N}_\lambda^b(T_B)|}{|\vec{N}_\lambda^b(T_S)|} \right\} \quad (24)$$

since $|\vec{N}_\lambda^b(T_Q)|$ is negligible compared to $|\vec{N}_\lambda^b(T_S)|$

This procedure assumes that the reflectivity of the sample is not temperature dependent and in fact is the same at liquid nitrogen temperature as at ambient temperatures. This assumption appears correct for the emissivity of Krylon 1602 ultra-flat black paint. Figure 10 shows a plot of the emissivity of this material calculated from data collected for $T_Q =$ liquid temperature and $T_Q = 275.1$ K. It can be seen from this plot that the two values of the emissivity are nearly equal.

For a sample which is a poor thermal conductor problems arise in determination of T_Q if it is chosen to be some temperature other than an extremely low temperature. This problem will be discussed fully later.

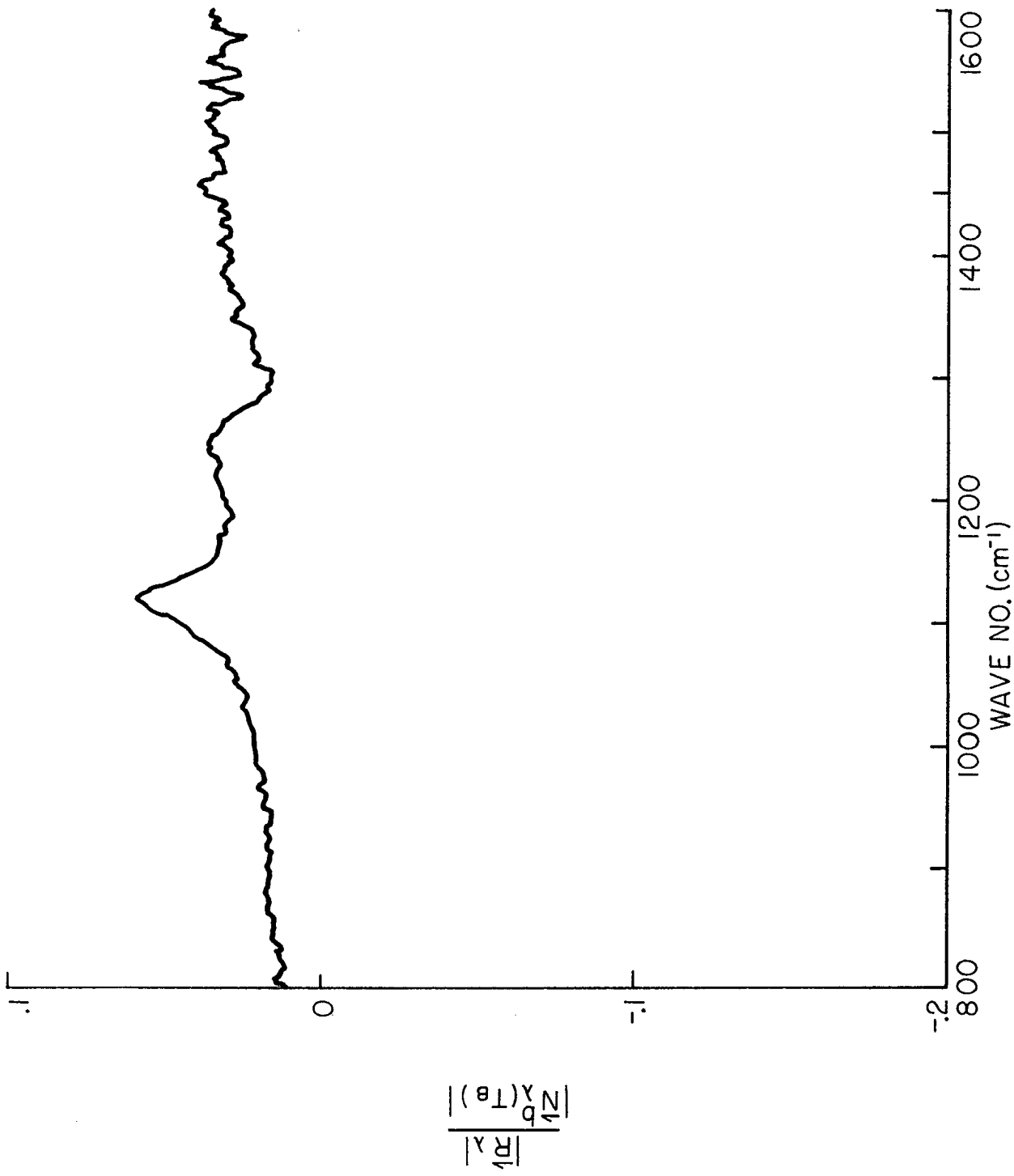


Fig. 9. Ratio of the reflectance term for fused quartz to blackbody radiation at 273 K.

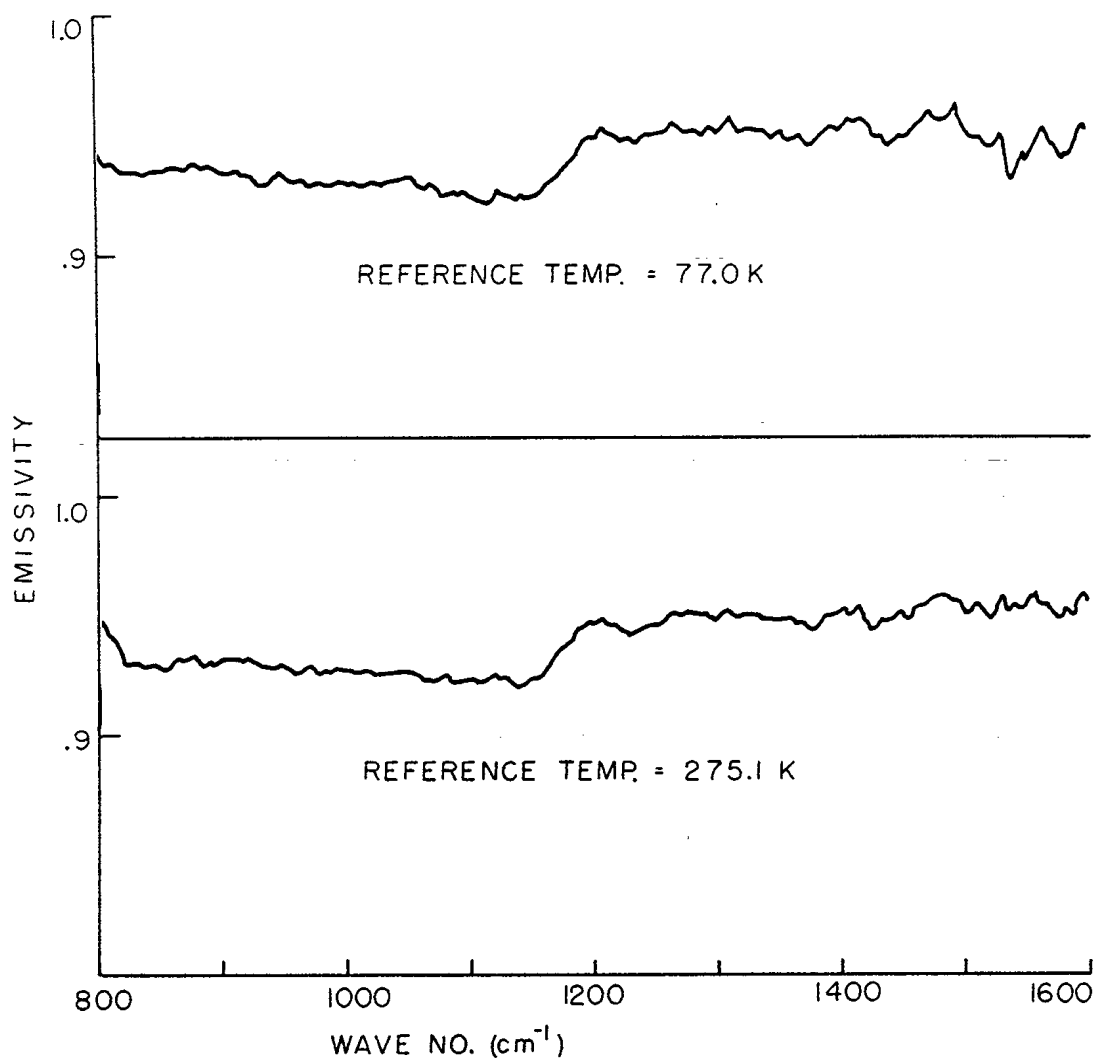


Fig. 10. Emissivity of Krylon 1602 ultra-flat black paint for $T_Q = 77$ K (top curve) and $T_Q = 275.1$ K (bottom curve).

SOFTWARE REQUIRED

The software obtained with the spectrometer and controlling computer is capable of doing the required mathematical operation on the term

$$\frac{|\vec{S}_\lambda(T_S) - \vec{S}_\lambda(T_Q)|}{|\vec{B}_\lambda(T_B) - \vec{B}_\lambda(T_L)|}$$

That is the subtraction can be carried out at the interferogram level, the fast Fourier transform applied with the appropriate apodization and phase error correction, and the result stored on disk in one of the available files.

It was necessary to write a program to calculate the blackbody ratio given by the second term in equation 22. This program was written in assembler language using the extended floating point package of Data General. The program accepts temperature inputs correct to a tenth of a degree for T_S , T_B and T_Q and calculates the required ratio of blackbody terms as a function of wave number. The term $|\vec{S}_\lambda(T_S) - \vec{S}_\lambda(T_Q)|$ of equation 22 is then modified by this blackbody ratio and the result is stored back into the original file location of $|\vec{S}_\lambda(T_S) - \vec{S}_\lambda(T_Q)|$. This program and auxiliary programs developed to do specialized operations on the data which can not be done by the DIGILAB software are either stored on disk in high sector number locations or on magnetic tape. This makes it possible to call any auxiliary program easily from the DIGILAB system, perform the calculation, and then transfer control back to the operating system.

COLD BOX PROFILE FUNCTION

Another important quantity is the profile function of the spectrometer - cold box system. From equations 13, 14, 15 and 17 it can be shown that

$$\vec{K}_\lambda = |\vec{B}_\lambda(T_B) - \vec{B}_\lambda(T_L)| \frac{1}{|\vec{N}_\lambda^b(T_B)|} \quad (25)$$

A plot of this quantity is shown in figure 11. It can be seen from this plot that the 3 dB power points are at approximately 825 and 1360 cm^{-1} .

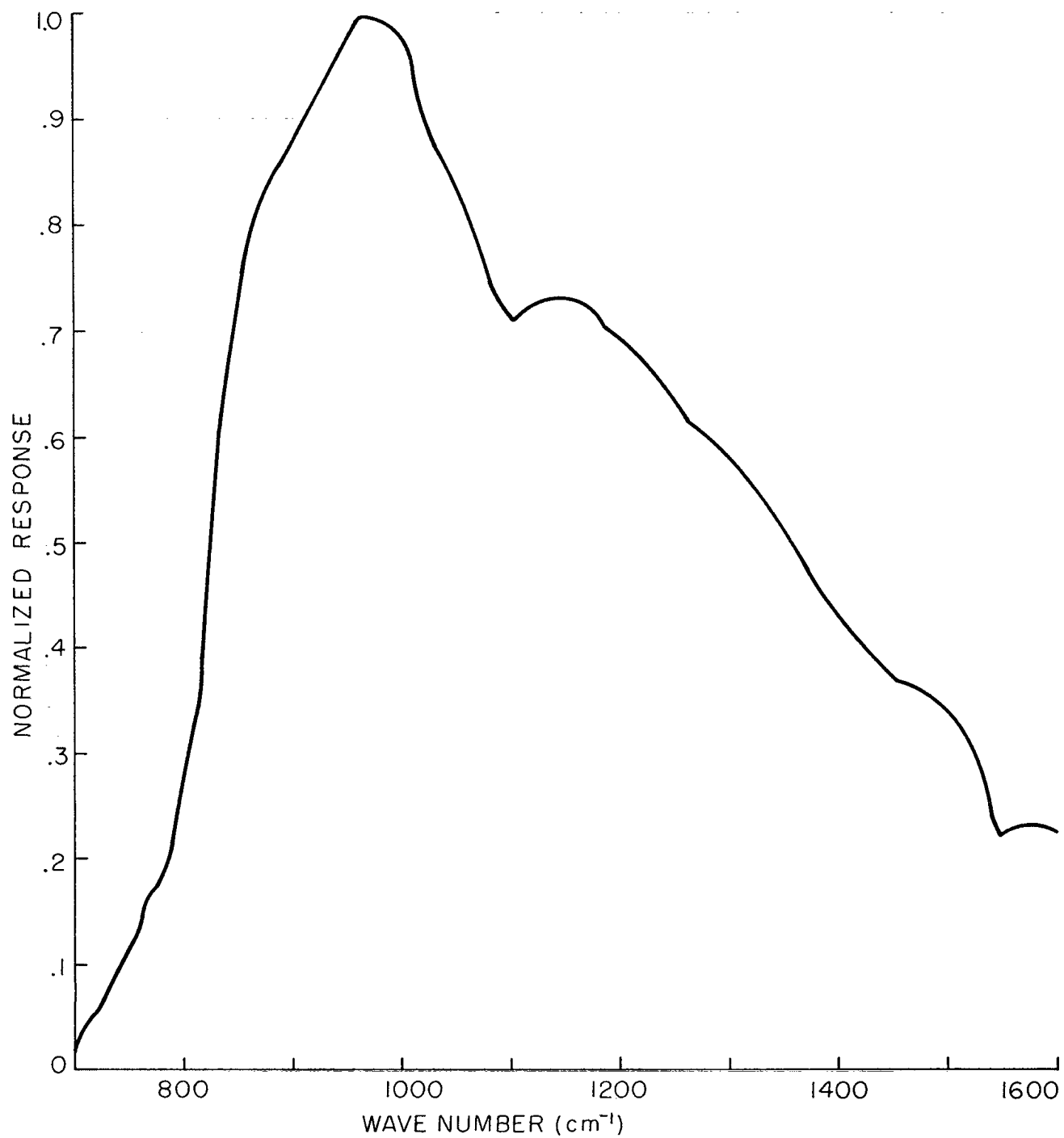


Fig. 11. Profile function of the spectrometer - cold box system.

OPERATING TECHNIQUES

DETERMINING EQUILIBRIUM TEMPERATURE

As mentioned previously, in order to maintain samples in a known thermal equilibrium state, the aluminum substrate, upon which the samples rest, should be maintained at the same temperature as the nitrogen gas above the sample. This eliminates any temperature gradients through the sample. This equilibrium temperature of the nitrogen gas above the sample was determined in the following manner.

First the insulated black source, was placed in the cold box sample holder and the system was allowed to come to a thermal equilibrium state which is dependent on the temperature of the manifold, the temperature of the cold box, and the rate of gas flow through the manifold. Because the styrofoam is a good thermal insulator the black painted surface should attain an equilibrium temperature which is not dependent on the environment conditions external to the cold box. The resulting spectrum which is recorded is given by equation 13.

$$\vec{S}_\lambda(T_S) = K_\lambda [\epsilon_\lambda \vec{N}_\lambda^b(T_S) + \vec{R}_\lambda + \vec{W}_\lambda] \quad (26)$$

where all the quantities are as defined in the previous section.

Next the black source was placed in the cold box. It is critical that this sample surface be at the same position in the cold box otherwise reflection and gas heating effects may differ. The aluminum substrate was maintained at some known temperature T_A and a second interferogram $\vec{S}_\lambda(T_A)$ was recorded. This is written as

$$\vec{S}_\lambda(T_A) = K_\lambda [\epsilon_\lambda \vec{N}_\lambda^b(T_A) + \vec{R}_\lambda + \vec{W}_\lambda] \quad (27)$$

It should be noted that the reflectance terms in equations 26 and 27 are the same since both surfaces have been painted with the same Krylon 1602 black paint. Again it is assumed that the sample reflectivity is not temperature dependent.

Finally the interferogram of a blackbody at liquid nitrogen temperature $\vec{B}_\lambda(T_L)$, was recorded. This is characterized as

$$\vec{B}_\lambda(T_L) = K_\lambda \vec{W}_\lambda \quad (28)$$

Now from equations 26, 27 and 28

$$\frac{|\vec{S}_\lambda(T_S) - \vec{B}_\lambda(T_L)|}{|\vec{S}_\lambda(T_A) - \vec{B}_\lambda(T_L)|} = \frac{\epsilon_\lambda |\vec{N}_\lambda^b(T_S)| + |\vec{R}_\lambda|}{\epsilon_\lambda |\vec{N}_\lambda^b(T_A)| + |\vec{R}_\lambda|} \quad (29)$$

since $\vec{N}_\lambda^b(T)$ and \vec{R}_λ have the same phase. Or

$$\left\{ \frac{|\vec{S}_\lambda(T_S) - \vec{B}_\lambda(T_L)|}{|\vec{S}_\lambda(T_A) - \vec{B}_\lambda(T_L)|} \right\} \left\{ \frac{|\vec{N}_\lambda^b(T_A)|}{|\vec{N}_\lambda^b(T_S)|} \right\} = \frac{\epsilon_\lambda \frac{|\vec{R}_\lambda|}{|\vec{N}_\lambda^b(T_S)|}}{\epsilon_\lambda \frac{|\vec{R}_\lambda|}{|\vec{N}_\lambda^b(T_A)|}} \quad (30)$$

In equation 30 the temperature T_S is unknown. It is, however, determined in the following manner.

(a) The RHS of this equation is approximately one since

$$\frac{|\vec{R}_\lambda|}{|\vec{N}_\lambda^b(T)|} \ll 1 \quad (\text{see for example figure 9}). \quad \text{Hence } T_S \text{ on the LHS is varied so}$$

as to make the LHS equal one. This revised value for T_S is T_S^1 .

(b) Another interferogram was then collected from the heated black source at $T_A = T_S^1$ and the same variational procedure repeated to determine a second T_S^1 . This procedure was continued until $|T_S - T_S^1| < \delta$ for δ some predetermined small quantity.

TEST OF THE SYSTEM

TEMPERATURE GRADIENT ACROSS AN INSULATED SAMPLE

In order to test for a possible temperature gradient over the insulated paper source when it is in an equilibrium state within the cold box a 2-inch diameter aluminum disk embedded in a 3-inch long styrofoam cylinder, was placed in the cold box. The aluminum disk was painted with Krylon 1602 ultra-flat black paint and embedded in the styrofoam so that its upper surface was flush with the upper surface of the styrofoam. This sample was placed in the cold box so that its upper surface was at the same height with respect to the manifold as that of the insulated paper sample. When thermal equilibrium was reached an interferogram was recorded and the resulting power spectrum was compared with that obtained for the insulated black paper source. These two spectra agreed closely which implies that a small temperature gradient must exist across the surface of the insulated paper sample since there is a uniform temperature over the surface of the aluminum disk.

TOTAL SYSTEM TEST

As a test of the system consisting of spectrometer and sample container it was decided to calculate the ratio of the emission from two blackbodies held at temperatures T_1 and T_2 , where T_1 and T_2 were near ambient. The sample used was the cylindrical blackbody source with the grooved bottom.

First three interferograms were collected for the blackbody sample at temperatures T_1 , T_2 and liquid nitrogen temperature. As before this latter interferogram was collected in order to correct for the instrument background radiation. The ratio of these corrected spectra is given by:

$$\frac{|\vec{B}_\lambda(T_1) - \vec{B}_\lambda(T_L)|}{|\vec{B}_\lambda(T_2) - \vec{B}_\lambda(T_L)|} = \frac{|\vec{N}_\lambda^b(T_1)|}{|\vec{N}_\lambda^b(T_L)|} \quad (31)$$

A plot of the LHS of this equation is given in figure 12 and for comparison a plot of the theoretical ratio for temperatures T_1 and T_2 (Planck's formula) is given. It can be seen from these curves that the agreement is within 1% over the region of interest.

TEMPERATURE GRADIENT BETWEEN THE SURFACE OF AN INSULATION SAMPLE
AND THE ALUMINUM SUBSTRATE

In order to determine the error which results by assigning to an insulated sample surface the temperature of the aluminum substrate when this substrate is kept at a temperature different from the equilibrium temperature above the sample, a crushed fused quartz sample was run at a substrate temperature 40 K greater than the nitrogen gas temperature above the sample. That is, the aluminum substrate temperature was changed but the temperature of the manifold and the rate of gas flow through it were not. The resulting expression for the emissivity was then considered to be a function of the surface temperature. This parameter was then varied by computer until the calculated emissivity agreed with the value obtained.

When the surface temperature was known, it was found that the actual surface temperature determined by this variation method was 5 to 10 K less than the substrate temperature.

This test shows very vividly one of the problems involved in determining the emissivity of an insulating sample. It was earlier established that it is necessary to record two interferograms of the sample at two different sample temperatures in order to subtract out the reflection term (see for example equation 18). During the recording of both of these interferograms the background must remain constant and hence the temperature of the manifold must be maintained at some fixed temperature. However, if this is done, and the substrate temperature is changed, it is not possible to assign a temperature to the surface with confidence. Hence the procedure has been adopted of choosing one of the sample temperatures to be that of liquid nitrogen which can be attained easily. Since at this low temperature

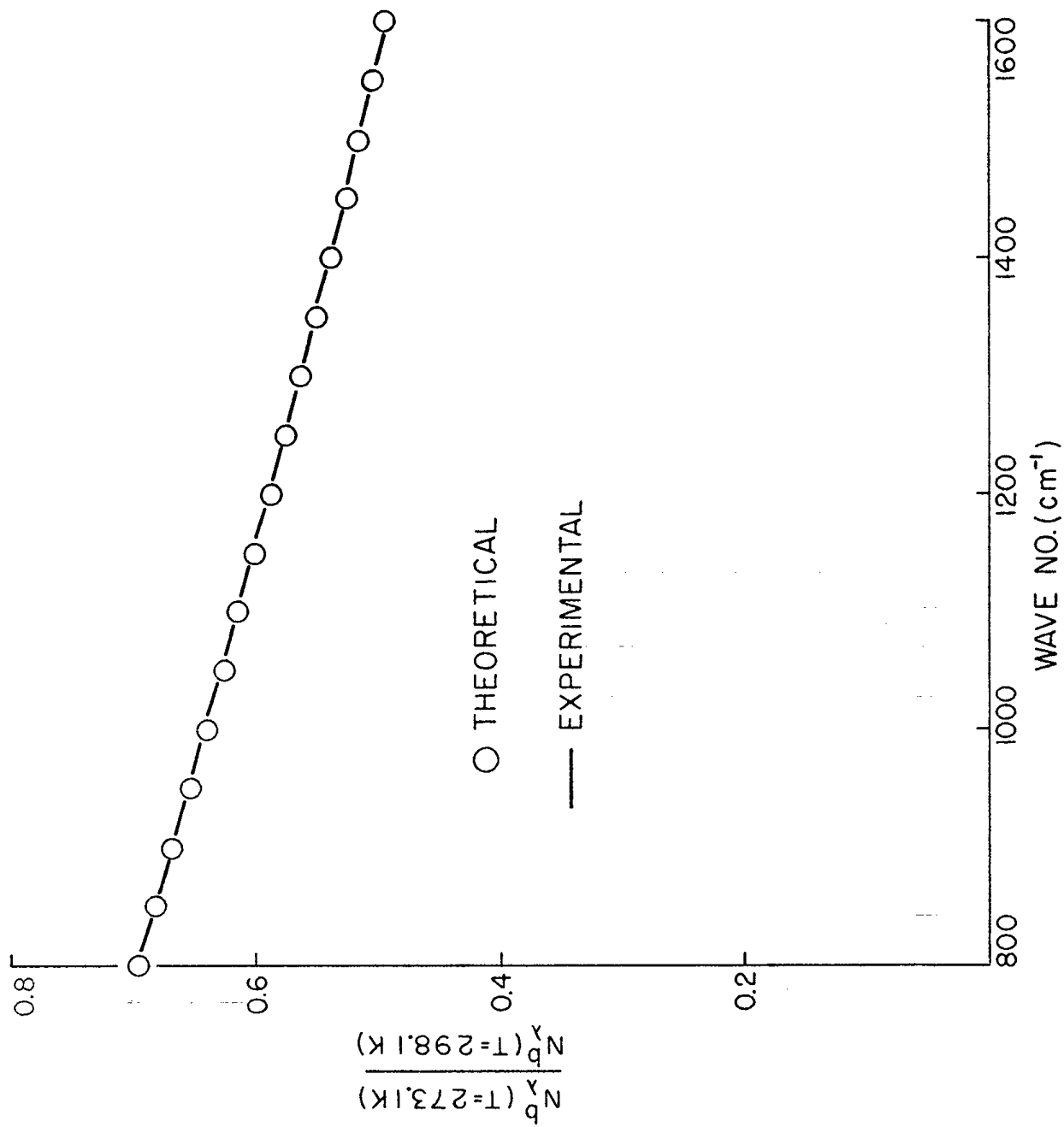


Fig. 12. Theoretical and measured ratio of two blackbodies at temperatures of 273.1 and 298.1 K.

the emission from the sample is negligible compared to the other terms contributing to the signal, a small error in the actual surface temperature produces a negligible error in the recorded interferogram.

RESULTS

GENERAL

The results of emissivity calculations were obtained for three materials at ambient temperature. The samples which have been considered are:

- (a) Krylon 1602 ultra-flat black paint
- (b) Crushed fused quartz (G.E. #204)
- (c) Three types of cotton
 - i) white duck 10 oz. (No. 20)
 - ii) navy blue 9.5 oz. (3/1 twill)
 - iii) olive drab drill 8.5 oz.

All the data which is presented in this report was collected by adding coherently the results of 100 scans at a resolution of 8 cm^{-1} . Data was not collected at a resolution of 1 cm^{-1} because our initial trials were intended to verify procedures rather than collect high resolution data. In addition, in all cases, box-car apodization was used in the Fourier transform and the phase function was computed by considering 64 points on either side of the central maximum of the interferograms.

KRYLON 1602 ULTRA-FLAT BLACK PAINT

SPECIMEN PREPARATION

This sample was prepared by first sandblasting one end of a cylindrical aluminum sample holder which was described earlier. The sandblasted surface was washed with acetone and two coats of the Krylon paint were applied from an aerosol can. The first coat was allowed to dry approximately ten minutes before the second coat was applied. This was sufficient for the first coat to become dry to the touch. The sample was then allowed to dry for about 24 hours before it was placed in the cold box and a spectrum recorded.

KRYLON EMISSIVITY

Figure 10 shows a plot of the emissivity of the Krylon 1602 ultra-flat black paint for a surface temperature of 275.1 K. This result may be compared

to reflectance measurements quoted by Strong (0.94 to 0.925 compared to 0.98 to 0.99) Some of this discrepancy may be due to the different modes of measurement. The values quoted by Strong were calculated from specular reflectance measurements at normal incidence angle and hence the effect of surface roughness should differ from our situation where emission into a finite solid angle is being considered.

Consequently, from our emissivity measurement, it can be seen that it is not possible to assume that a surface painted with Krylon 1602 paint is a blackbody without introducing errors of 5% to 7%.

CRUSHED FUSED QUARTZ

SAMPLE PREPARATION

This sample was prepared by crushing some G.E. #204 fused quartz. The resulting particles were then separated with a sieve so that only those with diameters in the range between .351 and .589 mm were kept. These particles were washed in dilute nitric acid, in distilled water, then acetone and finally dried on a hot plate at temperatures less than 373 K. This sample was then placed in a holder on one of the heated aluminum sample substrates (figure 8) to a depth of about 2 mm and an emission spectrum was collected.

EMISSIVITY OF CRUSHED QUARTZ

Figure 13 shows the emissivity for a sample at a temperature of 271.4 K. It can be seen from this plot that there is a very strong absorption peak (in this case a drop in the emissivity) at 1125 cm^{-1} ($8.88 \mu\text{m}$). This result is similar to that obtained by Hovis and Callahan (6) who measured the reflectance from G.E. #106 fused quartz samples. They found a very strong reflectance peak (30% to 40%) at about $9 \mu\text{m}$ for two samples; one made up of particles with diameters in the range 2 to 4 mm and the other with diameters between 0.015 and 0.20 mm. A third sample considered by Hovis and Callahan, made up of particles with diameters less than .038 mm, showed considerably less reflection at this wavelength of $9 \mu\text{m}$. This may be due to increased scattering of the incoming radiation due to the more random orientation of the particles.

Further, the spectral feature at 1225 cm^{-1} ($8.16 \mu\text{m}$) on our emissivity plot has a corresponding feature on the reflectance curves of Hovis and Callahan for the two samples with the larger sized particles. Lyon (11) has also found that quartz crystals and fused quartz exhibit depressions in the emissivity plots at $9.0 \mu\text{m}$.

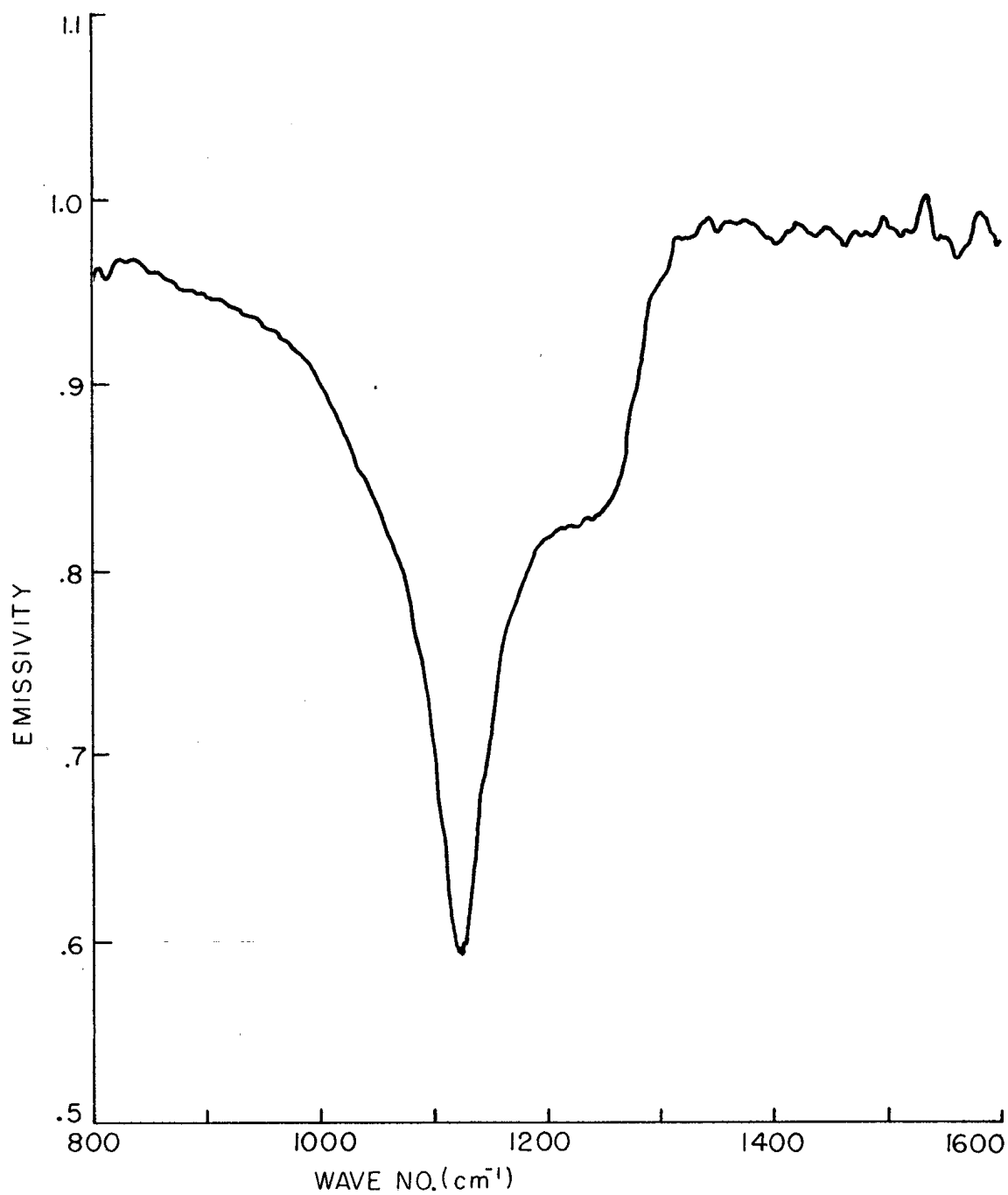


Fig. 13. Emissivity of a sample of crushed fused quartz (G.E. No. 204) at a temperature of 271.4 K.

COTTON

SAMPLE PREPARATION

The emission spectra of the cotton samples were measured using the cylindrical sample holder which was used to measure the emissivity of Krylon paint. In this case the end of the cylinder was cleaned with acetone and a circular piece of cotton was glued to the surface with rubber paper cement.

EMISSIVITY OF COTTON

Figure 14 shows the emissivities of the white, blue and olive drab cotton samples. It can be seen that these curves contain the same general spectral features although the relative magnitudes of them differ.

From figure 15, which is a plot of the ratio of these emissivities to one another, it can be seen that the olive drab and blue cotton samples are quite similar but they differ from white cotton especially in the wave number interval from 800 to 980 cm^{-1} . It appears that the reflectance of the blue and the olive drab samples is higher in this wave number interval than that of the cotton sample.

CONCLUSIONS

(a) The work described in this report was largely concerned with determining whether the equipment met criteria established for measuring spectral emissivity at ambient temperatures in the field, establishing the sample environment and sample handling techniques, and determining whether the available software was sufficient for the subsequent data analysis. It was concluded that the FTS-14 Fourier transform spectrometer by Digilab met the estimated criteria.

(b) The sample container, built and designed for laboratory control of the environment at the radiating surface of the sample, allows the thermal radiation from a sample at ambient temperature to be measured unambiguously.

(c) The techniques of measurement and analysis, developed to correct for background radiation within the spectrometer and for reflected radiation from the sample surface, work satisfactorily.

(d) The spectral emissivities measured for crushed fused quartz, cotton (olive drab, combat blue, and white), and Krylon 1602 ultra-flat black paint agree with the limited information in the literature and show that there are no major problems in developing a library of spectra on materials of interest. These measurements were made with the sample surface near average ambient temperature ($\approx 273 \text{ K}$) and over the spectral range of 800 to 1250 cm^{-1} with a spectral resolution of 8 cm^{-1} .

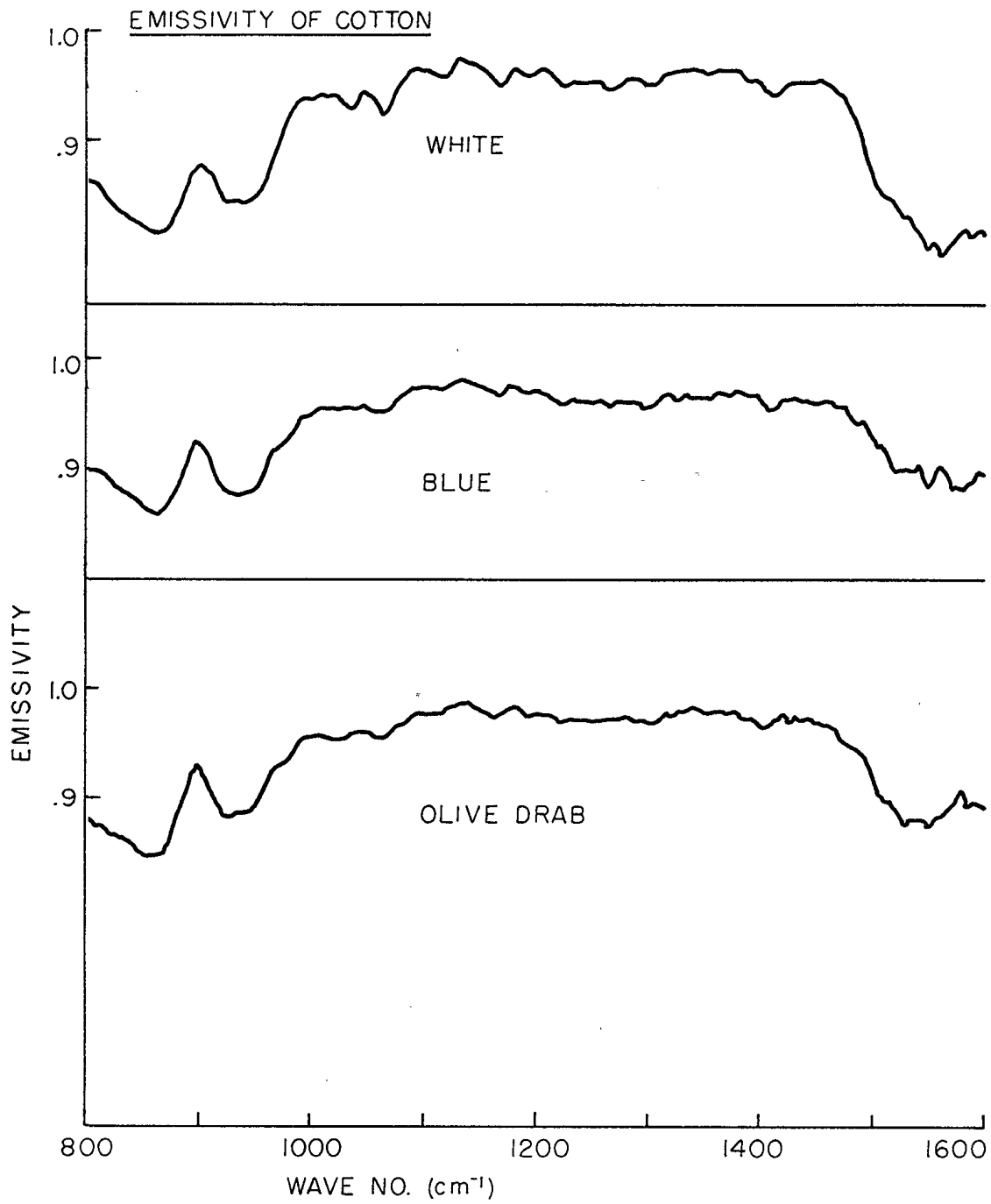


Fig. 14. Emissivity of white, blue, and olive drab cotton at ambient temperature.

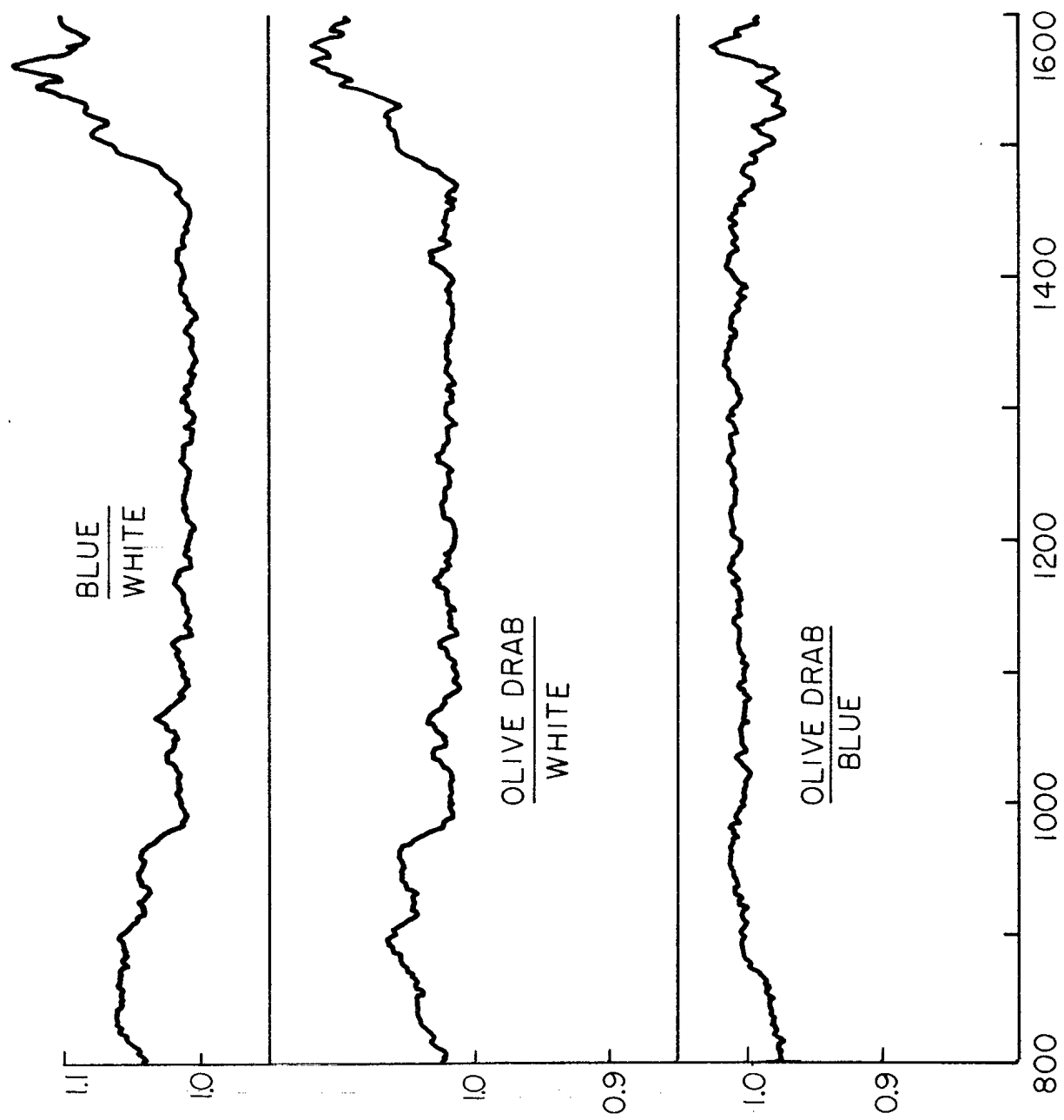


Fig. 15. Ratio of the emissivities of white, blue and olive drab cotton to one another.

REFERENCES

1. E.M. Zaitzeff, C.L. Korb, and C.L. Wilson, "MSDS: An Experimental 24 - Channel Multispectral Scanner System", IEEE Trans. Geosci. Electronics, GE-9, 114(1971).
2. H. Halpert and B.L. Musicant, "N-Colour (Hg.Cd)Te Photodectors", App. Opt. 11, 2157(1972).
3. J.R. Aronson and A.G. Emslie, "The Influence of Physical Variables on Spectral Signatures of Natural Objects", AFCRL - 70 - 0083, 1970.
4. R.D. Hudson, Jr., *Infrared Systems Engineering*, John Wiley and Sons, New York, 1969, p. 106.
5. R.J.P Lyon and E.A. Burns, "Analysis of Rocks and Materials by Reflected Infrared Radiation", Econ. Geol. 58, 274(1963).
6. W.A. Hovis, Jr., and W.R. Callahan, "Infrared Reflectance of Igneous Rocks, Tuffs and Red Sandstone from 0.5 to 22 μm ", J. Opt. Soc. Am. 56, 639(1966).
7. R.D. Watson, "Spectral Reflectance and Photometric Properties of Selected Rocks", Remote Sensing of Environment 2, 95(1972).
8. G.R. Hunt, J.W. Salisbury, and C.J. Lenhoff, "Visible and Near-Infrared Spectra of Minerals and Rocks: IV Sulphides and Sulphates", Space Physics Laboratory, AFCRL, preprint, 1970.
9. L.J. Pierre, Jr., "Exploratory Study of the Infrared Characteristics of Surface Slicks", Appl. Opt. 12, 2035(1973).
10. G. Fabbri and P. Baraldi, "Infrared Emission Spectra of Solids", Appl. Spectrosc. 26, 593(1972).
11. R.J.P. Lyon, "Analysis of Rocks by Spectral Infrared Emission (8 to 25 Microns)", Econ. Geol. 60, 715(1965).
12. M.J.D. Low and I. Coleman, "The Measurement of Infrared Emission Spectra Using Mult-Scan Interferometry", Spectrochim. Acta 22, 369(1966).
13. Reference 4, Chapter 7.
14. R.A. Hanel *et al.*, "Mariner 9 Michelson Interferometer", Appl. Opt. 11, 2625(1972).
15. R.A. Hanel, B. Schlachman, D. Rogers, and D. Vanous, "Nimbus 4 Michelson Interferometer", Appl. Opt. 10, 1376(1971),
16. J.H. Shaw, "Determination of the Earth's Surface Temperature from Remote Spectral Radiance Measurements near 2600 cm^{-1} ", J. Atmos. Sci 27, 950(1970).

17. W.L. Smith *et al.*, "Nimbus - 5 ITPR Experiment", *Appl. Opt.* 13, 499(1974).
18. Reference 4, Chapter 2.
19. G.R. Hunt, and R.K. Vincent, "The Behaviour of Spectral Features in the Infrared Emission from Particulate Surfaces of Various Grain Sizes", *J. Geophys. Res.* 73, 6039(1968).
20. R.S. Vickers and R.J.P. Lyon, "Infrared Sensing from Spacecraft - A Geological Interpretation", AIAA Paper No. 67-284, AIAA Thermophysics Specialists Conference, New Orleans, April 1967.
21. M.A. Bramson, *Infrared Radiation - A Handbook for Applications*, Plenum Press, New York, 1968, p. 126.
22. G.M. Hale and M.R. Querry, "Optical Constants of Water in the 200 nm to 200 μ m Wavelength Region", *Appl. Opt.* 12, 555(1973).
23. Reference 4, Chapter 2.
24. R.L. Carter, "Vibrational Selection Rules in Solids", *J. Chem. Educ.* 48, 297(1971).
25. *Aspen International Conference on Fourier Spectroscopy, 1970*, editors G.A. Vanasse, A.T. Stair, Jr., and D.J. Baker, AFCRL - 71 - 0019, January 5, 1971, Special Reports, No. 114.
26. R.A. Hanel, "Advances in Satellite Radiation Measurements", *Advan. Geophys.* 14, 377(1970).
27. A.T. Stair, Jr., Reference 25, p. 127.
28. P. Jacquinet, "The Luminosity of Spectrometers with Prisms, Gratings, or Fabry-Perot Etalons", *J. Opt. Soc. Am.* 44, 761(1954).
29. E.V. Loewenstein, "Fourier Spectroscopy: An Introduction", Reference 25, p. 3.
30. P. Fellgett, *On the Theory of Infrared Sensitivities and its Application to the Investigation of Stellar Radiation in the Near Infrared*, thesis, University of Cambridge (1951).
31. H. Sakai, "Consideration of the Signal-to-Noise Ratio in Fourier Spectroscopy", Reference 25, p. 19.
32. P. Hanson and J. Strong, "High Resolution Hadamard Transform Spectrometer", *Appl. Opt.* 11, 502(1972).
33. L. Mertz, *Transformations in Optics*, John Wiley and Sons, Inc., New York, 1965.

34. G.W. Chantry, *Submillimetre Spectroscopy*, Academic Press, London, 1971.
35. G.A. Vanasse, "The Michelson Interferometer Spectrometer", *Opt. Spectra* 4, 54(1970).
36. W.H. Steel, "Interferometers for Fourier Spectroscopy", Reference 25, p. 45.
37. Reference 34, Appendix 1.
38. A.G. Tescher, "Beam Splitter Optimization for Fourier Spectroscopy". Reference 25, p. 225.
39. "Standard Method of Test for Normal Spectral Emittance at Elevated Temperatures for Non-Conducting Specimens", 1973 Annual Book of American Society for Testing and Materials, Part 30, Section E423.
40. J. Strong, "Measurement of Radiation Flux", *Advan. Geophys.* 14, (1970), p. 309.
41. Unpublished design by F.G. Strain and built by J.D.R. Pattman, Defence Research Establishment Ottawa.
42. R. Bracewell, *The Fourier Transform and its Applications*, McGraw-Hill New York, 1965, Chapter 10.
43. J.W. Cooley and J.W. Tukey, "An Algorithm for the Machine Calculation of Complex Fourier Series", *Math. Comput.* 19, 296(1965).
44. J. Connes, "Computing Problems in Fourier Spectroscopy", Reference 25, p. 83.
45. G. Horlick and H.V. Malmstadt, "Basic and Practical Considerations for Sampling and Digitizing Interferograms Generated by a Fourier Transform Spectrometer", *Anal. Chem.* 42, 1361(1970).

4101U
4102U
4103U

42U

0201 DREO
0202 404576
0203 708

Unclassified

Security Classification

DOCUMENT CONTROL DATA - R & D	
(Security classification of title, body of abstract and indexing annotation must be entered when the overall document is classified)	
1. ORIGINATING ACTIVITY 0201a <u>DREO</u> - Ottawa; 0204b Ottawa ONT (CAN)	2a. DOCUMENT SECURITY CLASSIFICATION Unclassified
	2b. GROUP <u>NA</u>
3. DOCUMENT TITLE 04a A Procedure for Measuring Thermal Emission Spectra at Ambient Temperature <u>ced</u>	
4. DESCRIPTIVE NOTES (Type of report and inclusive dates) 08a Technical Report	
5. AUTHOR(S) (Last name, first name, middle initial) 1101 B.G. Young, and 1102 R.J. Brown, 07 CAN	
6. DOCUMENT DATE November 1979 46 Jan 75	7a. TOTAL NO. OF PAGES 09016055
	7b. NO. OF REFS 020245
8a. PROJECT OR GRANT NO. 35 D-38-80-07	9a. ORIGINATOR'S DOCUMENT NUMBER(S) <u>DREO Report No. 708</u>
8b. CONTRACT NO.	9b. OTHER DOCUMENT NO.(S) (Any other numbers that may be assigned this document) <u>N/A</u>
10. DISTRIBUTION STATEMENT Unlimited	
11. SUPPLEMENTARY NOTES	12. SPONSORING ACTIVITY <u>DREO</u>
13. ABSTRACT Unclassified <u>510</u> This report describes preliminary work to collect the infrared spectral emission signatures of ambient temperature objects using a Fourier transform spectrometer operating in the 8-13 micrometer wavelength range. Details of the construction of a sample container are presented along with a description of the spectrometer, the controlling computer, and the data collection techniques and procedures. A system test, which is actually the ratio of two blackbodies at different temperatures, suggests that these procedures are valid. The emissivities of Krylon 1602 ultra-flat black paint, crushed fused quartz, and three types of cotton are presented. //	

ml

KEY WORDS

Infrared emission spectra
Fourier transform spectrometer
Low temperature emission spectra

INSTRUCTIONS

1. ORIGINATING ACTIVITY: Enter the name and address of the organization issuing the document.
- 2a. DOCUMENT SECURITY CLASSIFICATION: Enter the overall security classification of the document including special warning terms whenever applicable.
- 2b. GROUP: Enter security reclassification group number. The three groups are defined in Appendix 'M' of the DRB Security Regulations.
3. DOCUMENT TITLE: Enter the complete document title in all capital letters. Titles in all cases should be unclassified. If a sufficiently descriptive title cannot be selected without classification, show title classification with the usual one-capital-letter abbreviation in parentheses immediately following the title.
4. DESCRIPTIVE NOTES: Enter the category of document, e.g. technical report, technical note or technical letter. If appropriate, enter the type of document, e.g. interim, progress, summary, annual or final. Give the inclusive dates when a specific reporting period is covered.
5. AUTHOR(S): Enter the name(s) of author(s) as shown on or in the document. Enter last name, first name, middle initial. If military, show rank. The name of the principal author is an absolute minimum requirement.
6. DOCUMENT DATE: Enter the date (month, year) of Establishment approval for publication of the document.
- 7a. TOTAL NUMBER OF PAGES: The total page count should follow normal pagination procedures, i.e., enter the number of pages containing information.
- 7b. NUMBER OF REFERENCES: Enter the total number of references cited in the document.
- 8a. PROJECT OR GRANT NUMBER: If appropriate, enter the applicable research and development project or grant number under which the document was written.
- 8b. CONTRACT NUMBER: If appropriate, enter the applicable number under which the document was written.
- 9a. ORIGINATOR'S DOCUMENT NUMBER(S): Enter the official document number by which the document will be identified and controlled by the originating activity. This number must be unique to this document.
- 9b. OTHER DOCUMENT NUMBER(S): If the document has been assigned any other document numbers (either by the originator or by the sponsor), also enter this number(s).
10. DISTRIBUTION STATEMENT: Enter any limitations on further dissemination of the document, other than those imposed by security classification, using standard statements such as:
 - (1) "Qualified requesters may obtain copies of this document from their defence documentation center."
 - (2) "Announcement and dissemination of this document is not authorized without prior approval from originating activity."
11. SUPPLEMENTARY NOTES: Use for additional explanatory notes.
12. SPONSORING ACTIVITY: Enter the name of the departmental project office or laboratory sponsoring the research and development. Include address.
13. ABSTRACT: Enter an abstract giving a brief and factual summary of the document, even though it may also appear elsewhere in the body of the document itself. It is highly desirable that the abstract of classified documents be unclassified. Each paragraph of the abstract shall end with an indication of the security classification of the information in the paragraph (unless the document itself is unclassified) represented as (TS), (S), (C), (R), or (U).

The length of the abstract should be limited to 20 single-spaced standard typewritten lines; 7½ inches long.
14. KEY WORDS: Key words are technically meaningful terms or short phrases that characterize a document and could be helpful in cataloging the document. Key words should be selected so that no security classification is required. Identifiers, such as equipment model designation, trade name, military project code name, geographic location, may be used as key words but will be followed by an indication of technical context.

4101W

42U

8901 a	<input checked="" type="checkbox"/>	11	Copy #	1
b	<input checked="" type="checkbox"/>	PD	ISSUED BY	
8902 a	<input checked="" type="checkbox"/>	DSIS/DIST.		
b				
c				
8903	<input checked="" type="checkbox"/>	MAR 4 1975	90	H
DSIS ACCN #		75-02252		
DEFENCE RESEARCH BOARD DEFENCE SCIENTIFIC INFORMATION SERVICE NATIONAL DEFENCE HEADQUARTERS OTTAWA, ONTARIO KIA 0Z3				

25555